Short title: Functions of CKXs in rice growth and development

Corresponding author: Chengqiang Ding (dingcq@njau.edu.cn)

Cytokinin oxidase/dehydrogenase family genes play important roles in the growth and development of rice[1]

Chenyu Rong,[a] Yuexin Liu,[a,2] Zhongyuan Chang,[a] Ziyu Liu,[a] Yanfeng Ding,[a,b,c] and Chengqiang Ding[a,b,c,3,4]

[a]College of Agriculture, Nanjing Agricultural University, Nanjing 210095, People's Republic of China

[b]Key Laboratory of Crop Physiology Ecology and Production Management, Ministry of Agriculture, Nanjing 210095, People's Republic of China

[c]Jiangsu Collaborative Innovation Center for Modern Crop Production, Nanjing 210095, People's Republic of China

[1]This work was supported by the National Natural Science Foundation of China (Grant number 31872855 and 31971842).

[2]Present address: National Key Laboratory of Crop Genetic Improvement, Huazhong Agricultural University, Wuhan 430070, People's Republic of China

[3]Senior author.

[4]Author for contact: dingcq@njau.edu.cn.

The author responsible for distribution of materials integral to the findings presented in this article in accordance with the policy described in the Instructions for Authors (www.plantphysiol.org) is: Chengqiang Ding (dingcq@njau.edu.cn).

One sentence summary: Cytokinin oxidase/dehydrogenase family genes exhibit functional divergence and overlap in rice growth and development.

Author contributions

C.D. and Y.D. conceived the original screening and research plans; C.R., Y.L., Z.C., Z.L., and C.D. performed the experiments and analyzed the data; C.R. and C.D. wrote the article with contributions of all the authors; C.D. agrees to serve as the author responsible for contact and ensures communication.

ABSTRACT

Cytokinin has important functions during plant growth and development; hence, many researchers have extensively studied cytokinin biosynthesis and degradation. Cytokinin oxidase/dehydrogenases (CKXs) are a group of enzymes that regulate oxidative cleavage to maintain cytokinin homeostasis. In rice, 11 *OsCKX* genes have been identified to date; however, most of their functions remain unknown. Here, we comprehensively analyzed the expression patterns of *OsCKX* genes and their genetic relationships using RNA sequencing (RNA-seq) and β-glucuronidase (GUS) staining. Using CRISPR/Cas9 technology, we constructed nine *osckx* mutants to determine the *OsCKX* function in rice development. Results revealed that each *OsCKX* gene has a unique expression pattern. Furthermore, the single *osckx* and higher-order *osckx4 osckx9* mutant lines showed functional overlap and subfunctionalization. Mutant phenotypes associated with decreased CKX activity exhibited changes in leaf and root growth, inflorescence architecture, fertilization, and grain weight. Notably, we found that the *osckx1 osckx2* and *osckx4 osckx9* double mutants displayed contrasting phenotypic changes in tiller number, culm diameter, and panicle size as compared to the wild-type (WT). Moreover, we identified several genes that were significantly expressed in *osckx4* and *osckx9* single and double mutant plants. Many differentially expressed genes, such as *OsPIN2*, *OsRR4*, and *OsNRT2.3*, were found to be associated with auxin, cytokinin, and nitrogen pathways. Therefore, our findings provide new insights on the functions of *OsCKX* genes in rice growth, that may be used as a foundation for future studies aimed at improving rice yield and initiating green production.

INTRODUCTION

Cytokinin controls plant growth and development by promoting plant cell division, growth, and differentiation. Specifically, it is responsible for stem enlargement and differentiation, organ development and structure, nutrition absorption, senescence, and stress response. Cytokinin biosynthesis starts from the ADP, ATP, or tRNA catalyzed by different adenosine phosphate isopentenyltransferases and activated by LONELY GUY enzymes (Kurakawa et al., 2007; Osugi et al., 2017). Previous studies reported that in rice, overexpression of adenosine phosphate isopentenyltransferase inhibited root formation (Sakamoto et al., 2006), while *lonely guy* mutants developed smaller panicles with reduced branches and floral organ defects (Kurakawa et al., 2007).

After performing its function, cytokinin is inactivated by certain enzymes such as cytokinin oxidase/dehydrogenases (CKXs) that induce cytokinin oxidative cleavage, which is an irreversible process. Cytokinin can also be inactivated by combining with sugars, including *O*-glucosyltransferase (reversible process) and *N*-glucosyltransferase (irreversible process) (Kudo et al., 2012). However, this inactivation process occurs at different stages of plant development in various tissues and employs several enzymes with similar functions, most of which remain unknown. CKXs are essential for maintaining cytokinin homeostasis during plant growth and development. Therefore, extensive research on CKXs has been conducted and is still ongoing. Each plant species has a group of *CKX* genes, for example, *Arabidopsis* has seven, rice has 11, and maize has 13. Most CKXs in maize and *Arabidopsis* have putative N-terminal secretory peptides that assist in locating the endoplasmic reticulum (ER) (Zalabak et al., 2016; Niemann et al., 2018). Previous studies have discovered several functions of CKXs in *Arabidopsis* and other crops. In *Arabidopsis*, overexpression of *AtCKX1* and *AtCKX2* resulted in smaller shoots, larger roots, and smaller shoot apical meristems (SAMs), while *AtCKX7* overexpression resulted in shorter primary roots (Werner et al., 2001; Kollmer et al., 2014). Furthermore, *ckx3 ckx5* mutants developed larger SAMs and more siliques (Bartrina et al., 2011). On the other hand, sextuple *ckx3*

ckx5 mutants of oilseed rape showed larger and more active inflorescence meristems (Schwarz et al., 2020). In barley, *HvCKX1* downregulation resulted in more spikes, more grains per spike, and higher 1,000-grain weight (Zalewski et al., 2010). *TaCKX6-D1* was found to be associated with grain filling and grain size in wheat (Zhang et al., 2012).

In rice, *OsCKX2/Gn1a* was the first *CKX* gene identified. Rice varieties with low *OsCKX2* expression yielded more grains per panicle, while *OsCKX2* downregulation or *osckx2* mutation produced more tillers, more grains per panicle, and heavier grains (Ashikari et al., 2005; Yeh et al., 2015). In contrast, *OsCKX4* overexpression reduced the tiller number, grain number per panicle, grain weight, and plant height and increased the number of roots (Gao et al., 2014). On the other hand, *osckx9* mutants developed more tillers and smaller panicles, while *OsCKX9* overexpression mutants displayed more tillers, shorter culms, smaller panicles, and lower setting rates (Duan et al., 2019). *OsCKX11* was found to regulate leaf senescence and grain number, while *osckx11* mutation resulted in the increased number of spikelets per panicle and tillers (Zhang et al., 2020). The expression of *CKX* genes is regulated by several transcription factors. For example, *OsCKX2* expression is controlled by zinc finger transcription factor DROUGHT AND SALT TOLERANCE and VIN3-LIKE 2 (Li et al., 2013; Yang et al., 2018), while the rice NAC family transcription factor OsNAC2 regulates *OsCKX4* expression (Gao et al., 2014; Mao et al., 2020).

OsCKX genes play an important role in the crosstalk between cytokinin and other hormones by regulating cytokinin content in plant tissues, maintaining plant hormone homeostasis, and controlling plant growth and development. Most *OsCKX* genes are upregulated by exogenous cytokinins, such as the naturally-occurring *trans*-zeatin (tZ) and N^6-(Δ^2-isopentenyl)adenine (iP) or the synthetic 6-benzylaminopurine (Duan et al., 2019). *OsCKX4* can also be induced by auxin, which plays a role in regulating the root system (Gao et al., 2014). The auxin response factor OsARF25 and the type-B response regulators ORR2 and ORR3 regulate the expression of

OsCKX4 downstream of auxin and cytokinin activation, respectively. However, *OsCKX4* overexpression can downregulate the expression of auxin-biosynthesis gene *OsYUCCA1* and auxin-transport genes *PIN FORMED1b* (*OsPIN1b*) and *OsPIN2* in the roots, showing the negative feedback between auxin and cytokinin. *OsCKX9* acts downstream of strigolactones (SLs) and plays a key role in the crosstalk between cytokinin and SLs. The SL-induced activation of *OsCKX9* relies on D53, which acts as a repressor of SL signaling and consequently functions in the SL-induced regulation of tiller development (Duan et al., 2019). On the other hand, *OsCKX11* has antagonistic roles between the cytokinin and abscisic acid (ABA) pathways during leaf senescence. In *osckx11* mutants, the downregulation of ABA biosynthesis genes and the upregulation of ABA degradation genes result in the reduction of ABA content in flag leaves and subsequently regulate leaf senescence, which shows the relationship between cytokinin and ABA. Thus, these findings demonstrate that *OsCKX* genes act as bridges between cytokinin and other plant hormones (Zhang et al., 2020).

OsCKX genes also respond to environmental changes and stressors. For example, high-concentration nitrogen treatment significantly increased *OsCKX* expression not only in nodes and leaves but also in young panicles (Ding et al., 2014; Xu et al., 2015), which also affected the tiller number and spikelets per panicle. Furthermore, *OsCKX1* and *OsCKX4* were found to be upregulated in nitrogen- and inorganic phosphate-starved roots, potentially affecting root system formation and assisting in the absorption of more nutrients (Shin et al., 2018). *OsCKX4* also plays a role in zinc absorption (Gao et al., 2019), while *OsCKX2* downregulation facilitates the adaptation to saline stress (Joshi et al., 2018). However, it is unknown whether *OsCKX* genes play other roles during rice growth and development. In rice breeding, *OsCKX2* has been artificially selected from wild rice since ancient times and can be divided into alleles from different geographic distributions (Ashikari et al., 2005; Wang et al., 2015). Since most plants with downregulated *CKX* expression exhibit better phenotypes, researchers believed that *CKX* is a potential target to improve yield or to initiate another “Green Revolution” (Ashikari et al.,

2005; Chen et al., 2020; Jameson and Song, 2020). Numerous studies have analyzed the structures of and genetic relationships between *OsCKXs*. However, the expression patterns that may determine their functions during plant growth, especially of *OsCKXs* with similar amino acid sequences, are yet to be elucidated.

In this study, we investigated the genetic relationships and expression patterns of *OsCKX* genes using RNA sequencing (RNA-seq). We also evaluated the phenotypes of *osckx* single and double mutants produced using CRISPR/Cas9 technology to determine the function of different *OsCKX*s. We also analyzed the transcriptomes of the roots and shoot bases from Nipponbare (NIP), *osckx4*, *osckx9*, and *osckx4/9* mutants to identify the genes downstream of *OsCKX4* and *OsCKX9*. Our findings may provide new insights regarding the potential application of *OsCKX* genes for improving agricultural traits.

RESULTS

OsCKX family genes display different expression patterns

Similar to the findings of previous studies, the *OsCKX* phylogenetic tree consisted of four major clades (Figure 1A). *OsCKX1*, which is commonly expressed in the roots, flowers, and grains, and *OsCKX2* were grouped together in the first clade. The β-glucuronidase (GUS) staining results reveal that *OsCKX1* had high expression in the shoot base and top of axillary buds, but very low expression in the leaf blade (Figure 1B). On the other hand, *OsCKX2*, usually expressed at high levels in the leaf sheath and inflorescence, was found to be highly expressed in the lateral root primordium, leaf blade, shoot base and inflorescence. *OsCKX6*, *OsCKX7*, and *OsCKX10* were grouped together in the second clade and showed very low expression in all tissues. Thus, these genes were excluded from future analysis.

The third clade was composed of *OsCKX4*, *OsCKX5*, and *OsCKX9*. *OsCKX4*, which is generally strongly expressed in the vegetative organs, displayed extremely high expression in the roots and inflorescence. *OsCKX9*, generally expressed at low levels in all tissues, showed high expression in the leaf blade, and whole axillary buds. *OsCKX5*, usually highly expressed in all tissues, also exhibited high expression in the roots and leaves.

The fourth clade consisted of *OsCKX3*, *OsCKX8*, and *OsCKX11*. *OsCKX3*, which is expected to have the highest expression in the stem and young panicles, , was found to have high expression in the shoot base and young panicle . *OsCKX8*, commonly expressed at lower levels than *OsCKX3* in all vegetative organs, was highly expressed in the shoot base, flag leaf primordia, and inflorescence. Furthermore, *OsCKX11*, generally expressed at a higher level than *OsCKX3* and *OsCKX8* in all tissues, specifically in the reproductive-stage root and inflorescence, displaying high expression in the root, shoot base, and young inflorescence.

Cytokinins have many functions during plant growth and development in different organs, and the biodegradation of cytokinins in different periods or tissues can help plants accurately regulate their growth and

development. In rice, we found all of eight of the *OsCKX* genes expressed at the shoot base and inflorescence meristem at different stages and positions. However, each *OsCKX* gene was expressed in a distinct pattern. As described above, certain *OsCKX* genes were highly expressed in certain organs, and we also found some tissues with certain *OsCKX* gene expressed at low levels, such as *OsCKX1* and *OsCKX3*, which were expressed at very low levels in the roots and leaves, and *OsCKX2*, *OsCKX3*, and *OsCKX11*, which were expressed at very low levels in the flag leaf primordia. Additionally, we also determined the expression patterns of *OsCKX* genes in axillary buds: *OsCKX1* was expressed in the top, *OsCKX2*, *OsCKX3*, *OsCKX4* and *OsCKX5* were expressed in the base, and *OsCKX9* was expressed throughout the buds. These distinct expression patterns stimulated our interest in their functions.

OsCKX single mutants exhibit different phenotypes

RNA-Seq analysis and GUS staining assay provided a clear view of the expression levels of *OsCKXs*; however, functional characterization of these genes is still lacking. Previous studies suggested that the knockdown of specific *OsCKXs* may help improve rice production by influencing important agronomic traits, such as tillering, development of organs facilitating nutrition, and panicle phenotype. To confirm this hypothesis, we analyzed the phenotypes of nine *OsCKX* single mutants (except for *OsCKX6* and *OsCKX10*, which were expressed at very low levels during rice growth and development) created using the CRISPR/Cas9 system (Supplemental Figures S1 and S2; Supplemental Table S1).

Since leaf size affects the photosynthetic capacity of rice, we investigated this and discovered that the top three leaves in the *osckx1*, *osckx2*, *osckx8*, and *osckx11* mutants were distinctly longer and wider compared to those of Zhonghua 11 (Supplemental Figures S3–S5; Supplemental Table S2). The *osckx9* mutant also had distinctly longer last three leaves, but there was no change in width compared to Zhonghua 11. The leaf length and width of the other mutants did not significantly change (Supplemental Figures S4, A–D, and S5). On the

other hand, culm diameter and plant height are closely related to the lodging resistance of rice. We found that the diameters of the basal internodes in *osckx1*, *osckx2*, *osckx8*, and *osckx11* mutants were significantly wider than those in the wild-type (WT), while the *osckx3*, *osckx4*, and *osckx5* mutants had thinner basal internodes (Supplemental Figure S4, E and F). Furthermore, the *osckx3*, *osckx4*, and *osckx5* mutants showed significantly decreased plant height compared to others (Supplemental Figure S4, G and H).

The panicle number is determined by the tiller number per plant and has a significant effect on rice yield. In the field and pot experiments, the *osckx4* and *osckx9* mutants developed more tillers than the WT plants, which is consistent with the results of previous studies (Supplemental Figures S3B and S4, I and J; Supplemental Tables S2 and S3). Although the mutants produced more panicles per plant, the number of grains per panicle decreased, resulting in no significant change in yield (Supplemental Figure S6, A and B; Supplemental Table S2). In contrast, the *osckx2* mutant showed significantly reduced tiller number in both the 2019 and 2020 field and pot experiments (Supplemental Tables S2 and S3). On the other hand, no significant differences were observed in the tiller numbers of the other *osckx* mutants. Additionally, there was no significant change in the yield per plant of the *osckx* mutants, except for *osckx1* and *osckx11-1*, which had significantly improved production. In contrast, *osckx3-1*, *osckx3-26*, and *osckx4-6* had significantly low yields (Supplemental Figures S6, A and B). Despite this, we observed several agronomic traits that were improved in the mutants. For example, the *osckx1*, *osckx2*, *osckx7* and *osckx8* mutants presented heavier grain weight, while the *osckx11* mutant developed more spikelets per panicle (Supplemental Figure S6, E–H).

The *osckx1 osckx2* double mutants have significantly reduced tiller numbers

Since the phenotypes of *osckx1* and *osckx2* plants weresimilar, we created the new double mutant *osckx1/2*. In the T1 generation, we obtained enough plants of the *osckx1/2-19* line, which has 1-bp insertions in *OsCKX1* and *OsCKX2* (Figure 2A; Supplemental Figure S2). The *osckx1/2-19* mutant showed significantly reduced tiller

number per plant (Figure 2B), consequently leading to lower panicle number per plant (Figure 2C). Notably, the *osckx1/2-19* mutants have large panicle sizes and more spikelets per panicle because the number of primary branches increased while the number of secondary branches remained the same (Figure 2, D–G). Furthermore, the 1,000-grain weight and grain length were significantly increased in *osckx1/2-19* compared with those in NIP (Figure 2H– J). In contrast, the grain width and thickness did not show significant changes between *osckx1/2-19* and NIP (Figure 2, I, K, and L). However, the total number of panicles and setting rate were lower in *osckx1/2-19* compared to those in NIP (Figure 2M), which resulted in a lower yield with no significant differences (Figure 2N). Overall, the *osckx1/2-19* plants showed better plant architecture than the WT. In *osckx1/2-19* plants, the flag leaf became wider (Figure 2, O and P) and the plants had thick basal internodes, while the plant height did not noticeably change (Figure 2, Q and R). Considered together, these observations suggest that the double knockout of *OsCKX1* and *OsCKX2* may have improved the lodging resistance and optimized plant architecture in rice.

Double knockout of *OsCKX4* and *OsCKX9* significantly promotes tillering

Since the *osckx4* and *osckx9* single mutants developed more tillers, we created two new single mutants, namely *osckx4-6* and *osckx9-1*, and an *osckx4/9* double mutant in NIP to verify if these will also produce more tillers (Supplemental Figure S7, A and B). As expected, we discovered that the *osckx4/9* double mutant had an extremely higher tiller number compared to NIP and the two single mutants (Figure 3, A–D). In contrast, panicle size was significantly reduced in the *osckx4/9* mutant (Figure 3E). The *osckx9-1* mutant had a high panicle number per plant, but the number was markedly higher in the *osckx4/9* mutant (Figure 3F). However, the number of spikelets per panicle of *osckx4* was significantly decreased, while that of *osckx4/9* was even lower (Figure 3G). The decreased number of spikelets per panicle of *osckx4-6* was due to the low number of secondary branches per panicle, while the low number of spikelets per panicle of *osckx4/9* was caused by the reduced number of both the

primary and secondary branches (Figure 3, E, H, and I). On the other hand, seed setting rates were similar in the single and double mutants, and were significantly lower than those in WT (Figure 3J). Despite the increase in grain length, the *osckx4-6* mutant presented decreased 1,000-grain weight due to reduced grain thickness (Figure 3K; Supplemental Figure S7, C–G). The 1,000-grain weight of *osckx4/9* was lower than that of the *osckx4-6* mutant due to reduced grain width and thickness (Figure 3I; Supplemental Figure S7). As a result of these changes, the yield of *osckx4/9* was significantly decreased (Figure 3L). Moreover, the root length, diameter of basal internode, plant height, and flag leaf length and width were further decreased in the double mutant compared to those in the two single mutants (Figure 3, A, M and N; Supplemental Figure S7, H–J).

We also conducted a hydroponic experiment to investigate the root phenotypes of the mutants (Figure 4A). We verified that *OsCKX4* and *OsCKX9* have redundant roles in regulating tillering, plant height, and root length (Figure 4 B and C). The *osckx4/9* mutant not only had shorter roots, but also fewer crown roots and smaller root diameter (Supplemental Figure S8, A and B). The length and width of the 8th leaf were also decreased in *osckx4-6* and *osckx4/9* compared to those in NIP (Figure 4, D and E). These results indicate that the reduction in the leaf size of *osckx4/9* started at the vegetative stage. Overall, these results suggest that *OsCKX4* and *OsCKX9* have a functional overlap during rice growth and development.

RNA-seq analysis reveals the molecular functions of *OsCKX4* and *OsCKX9*

To elucidate the functions of *OsCKX4* and *OsCKX9*, we sampled the roots and shoot bases from NIP, *osckx4*, *osckx9*, and *osckx4/9* and performed RNA-seq analysis. Results revealed that *osckx4* had 297 differentially expressed genes (DEGs) in the shoot bases and 415 DEGs in the roots. There were 500 DEGs in the shoot bases and 342 DEGs in the roots of the *osckx9* mutant. The *osckx4/9* double mutant had the highest number of DEGs, with 806 DEGs in the shoot base and 4,556 DEGs in the roots (Figure 5A). To verify the accuracy and reproducibility of the RNA-seq results, we randomly selected seven previously studied genes associated with the

phenotypes observed in this study for quantitative reverse-transcription PCR analysis. The expression profiles of these genes were found to corroborate the RNA-seq results (Supplemental Figure S9).

However, although there were numerous DEGs between the WT and mutants, there were 71 DEGs in the roots and 90 DEGs in the shoot bases that overlapped between the *osckx4* vs. WT and *osckx9* vs. WT comparisons and occupied only a small fraction of the total DEGs (Figure 5B). These included some genes that regulate the absorption of silicon (*Lsi1*, *Lsi2*), zinc (*OsZIP16*), and iron (*OsIRO2*) (Fig 5C). *OsZIP9*, *OsTCP19*, *OsHKT1;1*, and *OsNPF5.5* were upregulated in the shoots of *osckx4*, while *OsLBD37*, *OsARF19*, *OsMYB61*, and *MT1a* were upregulated in the shoots of *osckx9*. In the roots, the downregulation of *OsAAP5*, *OsAAP8*, and *OsNLP6* and the upregulation of certain genes influenced the iron and phosphorus absorption in *osckx4*. We also observed the downregulation of *OsPUP1*, *OsPUP5*, *OsRR10*, and *OsNAAT4* in *osckx9*. These DEGs were also revealed to be associated with the different pathways controlled by *OsCKX4* and *OsCKX9* (Figure 5C). However, the functions of most DEGs remain unknown (Supplemental Dataset 1). The difference in the number of DEGs identified may imply that *OsCKX4* and *OsCKX9* have different functions. Moreover, 87.1% and 78.2% of DEGs in the roots and shoot bases, respectively, between the *osckx4/9* and WT were identified only in the double mutants, which may have been caused by the duplicate effect of the functional loss of *OsCKX4* and *OsCKX9* (Figure 5B).

Since we observed that *osckx4/9* exhibited more severe phenotypes and possessed more DEGs, we analyzed the DEGs identified in the roots and shoot bases between the WT and *osckx4/9* plants by using Kyoto Encyclopedia of Genes and Genomes (KEGG) enrichment analysis (Figure 5D). In both tissues, the top enriched KEGG pathways included ‘glycolysis/gluconeogenesis,’ ‘biosynthesis of amino acids,’, and those related to carbon and nitrogen metabolism. Since most of the DEGs were not functionally annotated, the relationship between the DEGs and the enriched pathways and their influence on the growth and development of the mutant

plants were not fully understood. However, we identified several genes that may be associated with the phenotypes observed in this study.

OsCKX4 and _OsCKX9_ regulate the metabolism and transport of hormones

First, we identified genes related to gibberellin metabolism. We found that the expression of *OsKS1* and *OsKS2* was significantly downregulated in the roots of *osckx4/9* (Figure 6A; Supplemental Dataset 1). OsKS1 and OsKS2 are enzymes involved in gibberellin biosynthesis. The expression of *OsKS2* was downregulated in the roots of the *osckx9* mutant, while no changes were observed in the *osckx4* mutant. Other genes for GA biosynthesis and degradation, such as *GA20ox* and *GA2ox*, were markedly downregulated in the roots of the *osckx4/9* mutant. Some GA receptors were also downregulated in the roots of the *osckx4/9* mutant. The changes in the expression of gibberellin-related genes may explain the significantly reduced plant height of *osckx4/9* double mutants.

Further, we examined the genes associated with SLs to investigate the cause of the increased tiller numbers in the single and double mutants. We discovered that *OsD17* was downregulated 1.20-fold, which was not significant in the roots of *osckx4/9* (Figure 6B; Supplemental Dataset 1), this may have been the cause of the increased tiller number and another reason for reduced plant height of *osckx4/9*. However *OsD10* was upregulated 1.59-fold in the shoot base of *osckx4/9*, and *OsD17* was upregulated 1.38-fold in the shoot base of *osckx9*, neither of which reflect significant differences. This may have been caused by feedback regulation (Arite et al., 2007). Furthermore, the SL-related transcription factors *OsTB1* and *OsMADS57* were upregulated 1.28-fold and 1.03-fold, respectively, in the shoot bases of *osckx4*, neither of which were significant changes. Finally, *OsTB1* and *OsMADS57* were downregulated 1.71-fold and 2.29-fold in the roots of *osckx4/9*, and *OsMADS57* was downregulated 1.24-fold in the roots of *osckx9*, but their functions in roots remain unknown.

Additionally, investigation of several differentially expressed auxin-related genes revealed that auxin efflux

transporters *OsPIN2* and *OsPIN8* were upregulated in the shoot bases and the roots, respectively, of the mutants. We found that the auxin primary response genes *OsGH3-1*, *OsGH3-2*, *OsIAA9*, and *OsSAUR12* were upregulated in the shoot bases of the *osckx4/9* and single mutants. Additionally, *OsGH3-2*, nine *OsIAA* genes (*OsIAA1, 4, 9, 12, 14, 15, 19, 23, 24*), and five *OsSAUR* genes (*OsSAUR6, 20, 27, 28, 33*) were downregulated in the roots of *osckx4/9*; however, *OsIAA16* was upregulated in the roots of *osckx4/9*.

Furthermore, the functional loss of *OsCKX4* and *OsCKX9* also affected the expression of genes associated with cytokinin metabolism and signal transduction. The cytokinin-related genes *OsCKX2*, *OsCKX5*, *OsRR4*, *OsRR6*, *OsRR7*, *OsRR9*, and *OsRR10* were downregulated in the roots of *osckx4/9*, while *OsCRL4* was upregulated in the shoot bases of *osckx4/9* (Supplemental Dataset 1). These results may have been caused by the high cytokinin contents in the double mutants.

OsCKX4 and _OsCKX9_ are associated with nitrogen absorption

Many genes related to nitrogen absorption and assimilation, such as *OsNRT1*, *OsNRT2.2*, *OsNRT2.3*, *OsAMT1.3*, *OsNAR2.1*, and *OsNIR2*, were also discovered to be significantly upregulated in the roots of the *osckx4/9* mutant (Figure 7; Supplemental Dataset 1). In contrast, we observed the downregulation of *OsGS1;3* in the roots and that of *OsAS1* in the shoot bases of *osckx4/9*. Most of the genes related to nitrogen absorption and assimilation also showed similar trends in *osckx4*, while some did not show significant differences compared to NIP. However, *OsAMT3.2* and *OsGS1;3* were upregulated in the shoot bases of *osckx9*. The changes in the expression of these genes were significantly different from those of the *osckx4/9* double mutants. Several nitrate and peptide transporter (*OsNPF*) family genes were also found to be differentially expressed.

DISCUSSION

Functional differences and redundancy between *OsCKX* genes

To systematically determine the functions of *OsCKX* genes, we analyzed theirexpression patterns and investigated the phenotypes of *osckx* single and double mutants. Our study revealed the roles of most *OsCKX* genes in the growth and development of rice. After two years of field experiments, we discovered that *osckx4* and *osckx9* developed more tillers at the vegetative stage, while *osckx2* had fewer tillers. At the reproductive stage, the top three leaves were longer and wider and the basal internodes were thicker in *osckx1*, *osckx2*, *osckx8*, and *osckx11* (Zhonghua11 [ZH11] background), while wider flag leaves and thicker basal internodes were observed in *osckx1/2* (NIP background) (Figure 8). The *osckx9*, *osckx3*, *osckx4*, and *osckx5* mutants showed little changes in flag leaf length and width compared to their background, while *osckx3*, *osckx4*, and *osckx5* developed thinner basal internodes. For yield-related phenotypes, *osckx9* developed more panicles while *osckx9* and *osckx4* had fewer spikelets per panicle. Moreover, *osckx1*, *osckx2*, and *osckx8* displayed increased 1,000-grain weight, while *osckx11* showed reduced 1,000-grain weight.

Previous studies have described the functions of *OsCKX2*, *OsCKX4*, *OsCKX9*, and *OsCKX11*. First, researchers elucidated the function of *OsCKX2* after observing that null mutants or plants with downregulation of *OsCKX2* developed more spikelets per panicle (Ashikari et al., 2005), more tillers, and larger grains (Yeh et al., 2015). In the present study, we observed very little increase in the number of spikelets per panicle during the two-year field experiment, with the observed increase being lower than that observed by the other researchers. However, we found that the *osckx2* mutant of ZH11 showed significantly reduced tiller number within the first year of the field experiment. Another mutant, *osckx1/2* of NIP, also showed reduced tiller number, which supports the hypothesis that fewer tillers may be related to thicker culms. Furthermore, both the *osckx2* mutant of ZH and *osckx1/2* mutant of NIP presented increased 1,000-grain weight. The discrepancies between our results

and previous findings regarding panicle size may be attributed to the different cultivated varieties or environmental impact.

Furthermore, previous reports stated that *OsCKX4* overexpression can cause the development of a larger root system, but result in shorter plant height, fewer tillers, and smaller panicles (Gao et al., 2014). For example, *OsCKX4-RNAi* or *osckx4* mutants showed fewer crown roots and shorter root lengths (Gao et al., 2014; Mao et al., 2020). Since *OsCKX4* is commonly expressed in the root, previous studies were more focused on investigating the relationships between *OsCKX4* and the root system instead of the shoot system. Here, we discovered that *osckx4* mutants produced more tillers, especially at the early stages, but has fewer spikelets per panicle. Additionally, *osckx9* mutants have been reported to develop more tillers, fewer spikelets per panicle, and shorter plant height (Duan et al., 2019). Since the null mutations of *OsCKX4* and *OsCKX9* can affect the tiller number, we constructed *osckx4/9* mutants, which distinctly showed more tillers, shorter plant height, and smaller panicles. The increase in the tiller number of *osckx4/9* double mutants was greater than those observed in *osckx4* and *osckx9* single mutants. Furthermore, the decrease in plant height and number of spikelets per panicle of *osckx4/9* double mutants was also higher than those observed in *osckx4* and *osckx9* single mutants. These results suggest the partial functional overlap of *OsCKX4* and *OsCKX9* during rice growth and development. Moreover, *osckx11* mutants previously displayed more tillers, larger panicles, and lighter 1,000-grain weight (Zhang et al., 2020); these were also observed in our study. In general, we found that each *OsCKX* gene had its own function during rice growth and development as well as their own distinct characteristics, and each *osckx* single or double mutant had a distinct phenotype.

Potential causes of the functional differences and redundancy in *OsCKX* genes

The main function of CKX enzymes is the biodegradation of cytokinins. Previous studies have reported that CKXs catalyze different kinds of cytokinins. In maize, the ZmCKX enzyme activity has been systematically

analyzed, revealing that ZmCKX1 and ZmCKX12 specially targeted iP, tZ, and *cis*-zeatin (cZ). Furthermore, ZmCKX5 was partial to iP and isopentenyladenosine 5'-monophosphate, while ZmCKX2, ZmCKX3, ZmCKX4a, and ZmCKX4b preferred the biodegradation of iP-9-glucoside (iP9G) and cZ. Finally, ZmCKX8, ZmCKX9, and ZmCKX10 showed preference for tZ and cZ (Zalabak et al., 2014). In *Arabidopsis*, AtCKX1 showed the highest preference for tZ phosphates, iP phosphates, and iP9G, while AtCKX3 preferred iP phosphates and iPR, and AtCKX7 preferred iP9G and tZ (Kowalska et al., 2010). However, little is known about the preference of OsCKX enzymes, except OsCKX9 that is partial to tZ and OsCKX11 that specially targets tZ and cZ (Duan et al., 2019; Zhang et al., 2020). OsCKX11 has the same substrate as its homolog protein, ZmCKX10, while other OsCKX enzyme substrates may need to be inferred from endogenous hormone content data. Therefore, the distinctive functions of OsCKXs may be caused by their different target substrates.

CKX proteins are mainly localized in the ER because most contain an N-terminal signal peptide sequence (Zalabak et al., 2016; Niemann et al., 2018). In the ER, cytokinins combine with their receptors and initiate signaling transduction, while most ER-localized CKXs regulate cytokinin concentrations to precisely adjust cytokinin signals (Niemann et al., 2018; Romanov and Schmulling, 2021). Previous studies revealed that OsCKX4 and OsCKX11 are localized in the cytosol, while OsCKX9 is localized in the cytosol and nuclei (Gao et al., 2014; Duan et al., 2019; Zhang et al., 2020). These three CKXs potentially regulate the cytokinin balance in other cellular organelles. However, the locations of the remaining OsCKXs remain unknown. Hence, we hypothesize that the subcellular localization of OsCKXs may also influence their functional differentiation.

In this study, the *OsCKX* genes exhibited different expression patterns. For example, *OsCKX1* and *OsCKX2* were expressed in the inflorescences and grains, while *OsCKX4* was highly expressed in the roots. In summary, the differences in the nature of catalytic substrates, subcellular localization, and expression in tissues may contribute to the different functions observed in *OsCKX* family genes.

Significantly altered transcriptome of the *osckx4 osckx9* mutant

Although *OsCKX4* and *OsCKX9* have been extensively studied, we observed new phenotypes in the single mutants, which have not been reported previously. Interestingly, these two genes were found to exhibit redundant functions during rice growth and development. Hence, we first investigated the genes associated with plant height and then identified the DEGs related to gibberellin metabolism between the NIP and mutants. *OsKS1* and *OsKS2*, which encode enzymes that catalyze the second step of the GA biosynthesis pathway (Ji et al., 2014; Tezuka et al., 2015), were significantly downregulated in the roots of *osckx4/9*. On the other hand, possibly due to the limited substrate, the expression of several *GA20ox* and *GA2ox* genes for gibberellin biosynthesis and biodegradation, respectively, were downregulated in *osckx4/9*. We hypothesize that the disrupted biosynthesis of gibberellin may have caused the reduction in *osckx4/9* plant height. However, the mechanism by which *OsCKX4* and *OsCKX9* regulate the expression of *OsKS1* and *OsKS2* is unknown.

Since the double mutants exhibited semi-dwarf phenotypes with more tillers, we believed that the expression of SL-related genes may have changed in the double mutants. However, we did not observe any changes in the expression of SL-signaling genes but found that *OsD17* was downregulated in the roots of *osckx4/9* mutants. This contradicts a previous report that stated *d17* mutants developed dwarf plants and more tillers (Zou et al., 2005). On the other hand, the SL-related transcript factors *OsTB1* and *OsMADS57* were only downregulated in the roots. Furthermore, *OsTB1* was upregulated in the shoot bases of *osckx4*. Previous studies on *tb1* mutants and *OsMADS57* overexpression showed that these plants developed more tillers than the WT (Takeda et al., 2003; Guo et al., 2013). Since SL directly activates *OsCKX9* to regulate shoot architecture in rice, we also determined whether *OsCKX4* and *OsCKX9* can regulate the tiller number phenotype through the SL pathway by analyzing the expression of SL-related genes between WT and mutants. Based on these findings, cytokinin may be located downstream of the SL pathway during rice tillering. During the outgrowth of tiller buds,

the auxin at the tip of the axillary bud is transported by auxin efflux carriers. In *Arabidopsis*, cytokinin response factors regulate *PIN* expression (Simaskova et al., 2015; Waldie and Leyser, 2018). Here, we found that *OsPIN2* was upregulated in the shoot bases of *osckx4* and *osckx4/9*. In rice, OsPIN2 transports auxins from the shoot to the root–shoot junction, and overexpression of *OsPIN2* results in the increased number of tillers (Chen et al., 2012). However, further research is needed to determine which cytokinin response factor regulates *OsPIN2*.

We also found that several type-A transcription factors, including *OsRR4*, *OsRR6*, *OsRR7*, *OsRR9*, and *OsRR10*, showed lower expression in the roots of *osckx4/9*. Some were downregulated in single mutants. However, these results were contradictory, since type-A RR genes are primary response genes for cytokinin signaling, while *OsRR4*, *OsRR9*, and *OsRR10* were previously found to be upregulated in *OsCKX4*-overexpression lines (Gao et al., 2014). Since *OsRR4*, *OsRR9*, and *OsRR10* share similar amino acid sequences (Tsai et al., 2012; Wang et al., 2019) and *osrr9 osrr10* mutant lines developed fewer spikelets per panicle and higher tolerance to saline stress, we hypothesized that *OsRR4*, *OsRR9*, and *OsRR10* may have important functions during the cytokinin-induced inhibition of root growth. In the present study, we observed the downregulation of *OsWOX11* (Zhao et al., 2009) and *OsMADS25* (Yu et al., 2015) in the roots of *osckx4* and *osckx4/9*, which may explain why *osckx4* and *osckx4/9* plants have smaller root systems. Furthermore, we discovered that *OsCKX4* and *OsCKX9* influence several genes related to nitrogen absorption and utilization, providing new potential targets for improving nitrogen usage efficiency in rice. However, the mechanisms underlying this process are unknown; hence, further research is still required.

Interestingly, in addition to the genes regulated by both *OsCKX4* and *OsCKX9*, we also identified several genes that are regulated by *OsCKX4* and *OsCKX9* individually. In summary, the similar amino acid sequences but different expression patterns of *OsCKX4* and *OsCKX9* enable them to functionally overlap in the regulation of some pathways, while also individually regulating specific pathways.

CONCLUSION

Our systematic analysis of 11 genes in the OsCKX family reveals their complex expression patterns in rice. A total of nine *OsCKX* mutants were produced using CRISPR/Cas9 technology. By examining the phenotypes of the mutants throughout the rice growth period, we determined the functions of specific *OsCKX* genes in plant development. In specific, we discovered that *OsCKX4* and *OsCKX9* inhibited tillering, while *OsCKX1* and *OsCKX2* promoted tillering. Consideredtogether, our findings establish a community resource for fully elucidating the function of *OsCKXs*, providing new insights that may be used for future studies to improve rice yield and initiate green production.

MATERIALS AND METHODS

Plant materials and growth conditions

Oryza sativa L. ssp. *japonica* (cultivars: NIP and ZH11) was the WT rice material chosen for this study. The mutants were comprised *osckx1/2*, *osckx3*, *osckx4*, *osckx5*, *osckx9*, and *osckx4/9* from NIP and *osckx1*, *osckx2*, *osckx7*, *osckx8*, *osckx9*, and *osckx11* from ZH11. The target for *osckx1/2* matches *OsCKX1* and *OsCKX2* completely, and has a 1-bp mismatch for *OsCKX11*. The sequencing results showed that the *osckx1/2-19* line had a 1-bp insertion in *OsCKX1* and *OsCKX2*, but no change was observed in *OsCKX11* (Supplemental Figure S2).

The rice plants were grown in a field in Danyang, Jiangsu Province, China (31.907° N 119.466° E). We used 300 kg/hm^2 nitrogen, 150 kg/hm^2 P_2O_5, and 240 kg/hm^2 K_2O as base fertilizers for the field experiment. For the pot experiment, in each pot, 4.28 g urea was added, while 1.92 g KH_2PO_4 and 1.49 g KCl were used during the whole growth period. For the hydroponic experiment, the nutrient solution was composed of 2 mM KNO_3, 2 mM NH_4Cl, 0.32 mM $NaH_2PO_4{\cdot}2H_2O$, 0.011 mM $MnCl_2{\cdot}4H_2O$, 0.0185 mM H_3BO_3, 0.0006 mM $Na_2MoO_4{\cdot}2H_2O$, 0.0014 mM $ZnSO_4{\cdot}7H_2O$, 0.0016 mM $CuSO_4{\cdot}5H_2O$, 0.3 mM $MgCl_2{\cdot}6H_2O$, 0.66 mM $CaCl_2$, and 0.0448 mM Fe(II)-EDTA (pH = 5.5–6). The plants were grown in climate chambers under long-day conditions (15 h light at 28 °C and 9 h dark at 24 °C) with a relative humidity of ~70% and treated for 20 days.

Plasmid construction for genetic transformation

To construct the mutants for research by using CRISPR/Cas9 technology, as previously described, each *OsCKX* gene was assigned one to two single guide RNA oligo targets by using CRISPR/Cas9 technology as previously described (Mao et al., 2013). The primers used for vector construction and genotyping are shown in Supplemental Table S1.

To construct *pOsCKX::GUS*, An upstream fragment of the *OsCKX*-encoding region (>3 kb) was amplified by PCR, and the resulting amplicon was excised with the corresponding restriction endonuclease and ligated into the *pCAMBIA1300::GUS* vector (Wang et al., 2020).

Analysis of GUS activity

The GUS reporter activity was assayed by histochemical staining using GUS Staining Kit (FCNCS, https://www.fcncs.com). Various tissues were collected from *pOsCKX::GUS* transgenic plants at each developmental stage. After dipping in the GUS staining solution, the samples were taken out and then incubated in the staining solution for 6–48 h at 37 °C in the dark. The samples were destained thrice with 70% ethanol in a water bath for 5 min. Images were taken using SZX16 microscope (Olympus, Tokyo, Japan; https://www.olympus-lifescience.com/en/).

Sampling, RNA extraction and gene expression analysis

We collected roots from 2 cm under the tip and shoot bases (~5-mm segments from the first nodes) containing the SAMs, axillary buds, young leaves, and tiller nodes from WT, *osckx4*, *osckx9*, and *osckx4/9* plants. The samples were stored at −80 °C until further use.

Total RNA was extracted using E.Z.N.A.® Plant RNA Kit (Omega Bio-tek Inc., Norcross, GA, USA; https://www.omegabiotek.com/) and subjected to reverse-transcription using PrimeScript™ RT Reagent Kit (Takara Biotechnology, Tokyo, Japan). Quantitative reverse-transcription PCR was performed on ABI PRISM 7300 Real-Time PCR System (Applied Biosystems, Thermo Fisher Scientific, Waltham, MA, USA; https://www.thermofisher.com/) with SYBR® Premix Ex Taq™ (Takara), following the manufacturer's instructions. Relative expression analysis was performed using the actin gene as internal control. The primers used are listed in Supplemental Table S1.

Sequence alignment and phylogenetic analysis

The amino acid sequence alignment was performed using MUSCLE (Madeira et al., 2019), and phylogenetic trees were generated using neighbor-joining method and 1,000 bootstrap iterations in MEGA X (Kumar et al., 2018).

RNA-Seq and data analysis

Before library preparation, oligo(dT)-attached magnetic beads (Invitrogen, Cat. No. 61006) were used to purify the mRNA. MGIEasy RNA Library preparation kit was used for library construction from purified mRNA according to the manufacturer's instruction (BGI, Cat. No. 1000006383). The quality of the constructed library is checked and sequenced after passing. High-throughput sequencing was paired-end sequenced on the BGISEQ-500 platform (BGI-Shenzhen, China). The obtained reads were processed and analyzed, and genes with *Q* values < 0.05 and fold change values > 1 were considered significantly differentially expressed. Based on the list of DEGs, we created and modified Venn diagrams in Microsoft Excel. Furthermore, we performed KEGG enrichment analysis ($Q < 0.05$) (Kanehisa, 2019), and generated a bubble chart using R.

ACCESSION NUMBERS

Sequence data from this article can be found in Rice Annotation Project database under the following accession numbers: *Actin* (Os03g0718100), *OsCKX1* (Os01g0187600), *OsCKX2* (Os01g0197700), *OsCKX3* (Os10g0483500), *OsCKX4* (Os01g0940000), *OsCKX5* (Os01g0775400), *OsCKX7* (Os02g0220100), *OsCKX8* (Os04g0523500), *OsCKX9* (Os05g0374200), *OsCKX11* (Os08g0460600), *OsMADS25* (Os04g0304400), *OsMADS57* (Os02g0731200), *OsD17* (Os04g0550600), *OsPIN2* (Os06g0660200), *OsWOX11* (Os07g0684900), *OsRR4* (Os01g0952500), *OsTB1* (Os03g0706500).

Supplemental data

The following supplemental materials are available.

Supplemental Figure S1. Gene structures and mutation details of *OsCKXs*.

Supplemental Figure S2. Chromatograms of the *osckx* mutant lines.

Supplemental Figure S3. The *osckx* mutants of Zhonghua11 from the 2020 field experiment.

Supplemental Figure S4. Phenotypic characterization of the vegetative organs in *osckx* mutants from the 2020 field experiment.

Supplemental Figure S5. Phenotypic characterization of the second and third top leaves in *osckx* mutants from the 2020 field experiment.

Supplemental Figure S6. Phenotypic characterization of yield-related phenotypes in *osckx* mutants from the 2020 field experiment.

Supplemental Figure S7. Mutation details of *OsCKX9*, chromatograms of the *osckx9* and *osckx4/9* mutant lines, and phenotypic characterization of the flag leaves and seeds in wild-type, *osckx4*, *osckx9*, and *osckx4/9* plants.

Supplemental Figure S8. Phenotypic characterization of the leaf and root systems in wild-type and *osckx4/9* plants.

Supplemental Figure S9. Relative expression levels and FPKM values of *D17*, *RR4*, *WOX11*, *PIN2*, *TB1*, *OsMADS25*, and *OsMADS57* in the roots and shoot bases (BP) of Nipponbare (NIP), *osckx4*, *osckx9*, and *osckx4/9*.

Supplemental Table S1. Information of primers used in the study.

Supplemental Table S2. Characterization of the vegetative organs and yield-related phenotypes in *osckx* mutants from the 2019 field experiment.

Supplemental Table S3. Tiller numbers in *osckx* mutants from the 2019 field experiment.

Supplemental Dataset 1. RNA sequencing data.

Acknowledgments

We thank Jiankang Zhu and Caixia Gao for providing the vectors of the CRISPR-Cas9 system. We also thank Biogle and Biorun genome editing center for producing transgenic rice.

FIGURE LEGENDS

Figure 1. Genetic relationship and expression patterns of *OsCKX* genes based on RNA sequencing data and GUS staining assay. A, Genetic relationship and expression patterns of *OsCKX* genes investigated in the leaf blade at the vegetative stage (LBV), leaf sheath at the vegetative stage (LSV), root at the vegetative stage (RV), leaf blade at the reproductive stage (LBR), leaf sheath at the reproductive stage (LSR), root at the reproductive stage (RR), stem (S), inflorescence meristem (IM), flower (F), and grain (G). The expression pattern was based on $\log_2$ Fragments Per Kilobase of exon model per Million mapped fragments (FPKM) values. B, Histochemical GUS staining of *pOsCKX::GUS* transgenic plants at various developmental stages. The scale bar in B was 1 mm.

Figure 2. Genetic and phenotypic characterization between wild-type (WT) and *osckx1/2-19* mutant plants. A, Mutation details of the coding sequences in the *OsCKX1* and *OsCKX2* of *osckx1/2-19* mutant. Both *OsCKX1* and *OsCKX2* had functional loss due to the 1-bp insertion caused by frameshift mutation. The solid yellow, blue, and red boxes represent the exons, untranslated regions, and target sequences, respectively. The introns are shown as solid lines, while protospacer adjacent motif (PAM) sequences are shown in red color and underlined with red. B, Number of tillers at the vegetative stage 70 days after sowing. C, Panicles at the reproductive stage (n = 20 for Nipponbare [NIP], n = 10 for *osckx1/2-19*). D, Panicle phenotypes of NIP and *osckx1/2* plants. The image was digitally extracted and scaled for comparison (scale bar = 10 cm). E–H, Measurement of the spikelets per panicle (E),

primary branches per panicle (F), secondary branches per panicle (G), 1,000-grain weight (H) (n > 20 for E–G, n = 5 for H) and *osckx1/2-19* (n > 10 for E–G, n = 5 for H) plants. I, Grain phenotypes of NIP and *osckx1/2* plants. The image was digitally extracted and scaled for comparison (scale bar = 1 cm). J-R, Measurement of the grain length (J), grain weight (K), and grain thickness (L) , seed setting rate (M), yield per plant (N), length of flag leaves (O), width of flag leaves (P), basal internode diameter (Q), and plant height (R) of NIP (n > 50 for J–L, n > 20 for M–Q) and *osckx1/2-19* ((n > 50 for J–L, n > 10 for M–Q) plants. The P-values indicate the significant differences between NIP and *osckx1/2-19* determined by Student's *t*-test.

Figure 3. Phenotypic characterization between wild-type (WT) and *osckx4*, *osckx9*, and *osckx4/9* mutant plants from the field experiment. A, Phenotypic features of Nipponbare (NIP), *osckx4*, *osckx9* and *osckx4/9* seedlings at the vegetative stage 46 days after sowing. The image was digitally extracted and scaled for comparison (scale bar = 10 cm). B–C, Number of tillers at the vegetative stage 46 days after sowing (B) and reproductive stage 70 days after sowing (C) (n > 20 for NIP, *osckx4-6*, and *osckx9-1*, n = 10 for *osckx4/9*). D–E, Habits (D) and panicle phenotypes (E) of NIP, *osckx4-6*, *osckx9-1*, and *osckx4/9* plants at the mature stage. The image was digitally extracted and scaled for comparison (scale bar = 10 cm). F–N, Measurement of the panicle number (F), spikelets per panicle (G), seed setting rate (H), 1,000-grain weight (I), yield per plant (J), plant height (K), primary branches per panicle (L), secondary branches per panicle (M), and diameter of basal internode of NIP (N), *osckx4-6*, *osckx9-1* (n > 20 for F–H and J–N, n = 5 for I), and *osckx4/9* (n > 10 for F–H and J–N, n = 5 for I). Different capital letters represent significant differences ($P < 0.01$) determined by one-way ANOVA and shortest significant ranges (SSR) test.

549 **Figure 4.** Phenotypic characterization between wild-type (WT) and *osckx4*, *osckx9*, and *osckx4/9* mutant plants
550 from the hydroponic experiment. A, Phenotypic features of Nipponbare (NIP), *osckx4*, *osckx9*, and *osckx4/9*
551 seedlings 21 days after transferring to hydroponic solutions. The image was digitally extracted and scaled for
552 comparison (scale bar = 10 cm). B–E, Measurement of the shoot and root lengths (B), tiller numbers (C), length
553 of 8^{th} leaf (D), and width of 8^{th} leaf (E) of NIP, *osckx4-6*, *osckx9-1*, and *osckx4/9* seedlings (n = 24 each).
554 Different capital letters represent significant differences ($P < 0.01$) determined by one-way ANOVA and SSR
555 test.
556
557 **Figure 5.** RNA-seq analysis of the roots and shoot bases (BP) between wild-type (WT) and *osckx4*, *osckx9*, and
558 *osckx4/9* mutant plants. A, The number of differentially expressed genes (DEGs) identified in the roots and shoot
559 bases of the following pairwise comparisons: Nipponbare (NIP) vs. *osckx4*, NIP vs. *osckx9*, and NIP vs. *osckx4/9*.
560 The changes in gene expression levels were calculated using the $\log_2$ fold change and Q values from three
561 biological replicates. B, Overlapping DEGs in the roots and shoot bases (BP) of NIP vs. *osckx4*, NIP vs. *osckx9*,
562 and NIP vs. *osckx4/9*. C, DEGs in *osckx4* and *osckx9* specifically and in commonin the roots and shoots, genes in
563 magenta are upregulated; genes in sky blue are downregulated. D, Top enriched Kyoto Encyclopedia of Genes
564 and Genomes (KEGG) pathways of the DEGs identified in the roots and shoot bases of NIP vs. *osckx4/9*.
565
566 **Figure 6.** *OsCKX4* and *OsCKX9* are associated with several signal transduction pathways. A, Differentially
567 expressed genes (DEGs) related to gibberellin metabolism and signaling transduction. B, DEGs related to
568 strigolactone biosynthesis and signaling transduction. * $Q < 0.05$, ** $Q < 0.01$.
569
570 **Figure 7. *OsCKX4* and *OsCKX9* associated with nitrogen absorption.** Differentially expressed

571 genes related to nitrogen absorption, metabolism, and transportation. * $Q < 0.05$, ** $Q < 0.01$.

572

573 **Figure 8. Patterns of *OsCKX* genes in rice.**

574 **Literature Cited**

575 Arite T, Iwata H, Ohshima K, Maekawa M, Nakajima M, Kojima M, Sakakibara H, Kyozuka J (2007)
576 DWARF10, an RMS1/MAX4/DAD1 ortholog, controls lateral bud outgrowth in rice. Plant J 51:
577 1019-1029
578 Ashikari M, Sakakibara H, Lin S, Yamamoto T, Takashi T, Nishimura A, Angeles ER, Qian Q, Kitano H,
579 Matsuoka M (2005) Cytokinin oxidase regulates rice grain production. Science 309: 741-745
580 Bartrina I, Otto E, Strnad M, Werner T, Schmulling T (2011) Cytokinin regulates the activity of reproductive
581 meristems, flower organ size, ovule formation, and thus seed yield in Arabidopsis thaliana. Plant Cell
582 23: 69-80
583 Chen L, Zhao J, Song J, Jameson PE (2020) Cytokinin dehydrogenase: a genetic target for yield improvement in
584 wheat. Plant Biotechnol J 18: 614-630
585 Chen Y, Fan X, Song W, Zhang Y, Xu G (2012) Over-expression of OsPIN2 leads to increased tiller numbers,
586 angle and shorter plant height through suppression of OsLAZY1. Plant Biotechnol J 10: 139-149
587 Ding C, You J, Chen L, Wang S, Ding Y (2014) Nitrogen fertilizer increases spikelet number per panicle by
588 enhancing cytokinin synthesis in rice. Plant Cell Rep 33: 363-371
589 Duan J, Yu H, Yuan K, Liao Z, Meng X, Jing Y, Liu G, Chu J, Li J (2019) Strigolactone promotes cytokinin
590 degradation through transcriptional activation of CYTOKININ OXIDASE/DEHYDROGENASE 9 in
591 rice. Proc Natl Acad Sci U S A 116: 14319-14324
592 Gao S, Fang J, Xu F, Wang W, Sun X, Chu J, Cai B, Feng Y, Chu C (2014) CYTOKININ
593 OXIDASE/DEHYDROGENASE4 Integrates Cytokinin and Auxin Signaling to Control Rice Crown
594 Root Formation. Plant Physiol 165: 1035-1046
595 Gao S, Xiao Y, Xu F, Gao X, Cao S, Zhang F, Wang G, Sanders D, Chu C (2019) Cytokinin-dependent
596 regulatory module underlies the maintenance of zinc nutrition in rice. New Phytol 224: 202-215
597 Guo S, Xu Y, Liu H, Mao Z, Zhang C, Ma Y, Zhang Q, Meng Z, Chong K (2013) The interaction between
598 OsMADS57 and OsTB1 modulates rice tillering via DWARF14. Nat Commun 4: 1566
599 Jameson PE, Song J (2020) Will cytokinins underpin the second 'Green Revolution'? J Exp Bot 71: 6872-6875
600 Ji SH, Gururani MA, Lee JW, Ahn BO, Chun SC (2014) Isolation and characterisation of a dwarf rice mutant
601 exhibiting defective gibberellins biosynthesis. Plant Biol (Stuttg) 16: 428-439
602 Joshi R, Sahoo KK, Tripathi AK, Kumar R, Gupta BK, Pareek A, Singla-Pareek SL (2018) Knockdown of an
603 inflorescence meristem-specific cytokinin oxidase - OsCKX2 in rice reduces yield penalty under
604 salinity stress condition. Plant Cell Environ 41: 936-946
605 Kanehisa M (2019) Toward understanding the origin and evolution of cellular organisms. Protein Science 28:
606 1947-1951
607 Kollmer I, Novak O, Strnad M, Schmulling T, Werner T (2014) Overexpression of the cytosolic cytokinin
608 oxidase/dehydrogenase (CKX7) from Arabidopsis causes specific changes in root growth and xylem
609 differentiation. Plant J 78: 359-371
610 Kowalska M, Galuszka P, Frebortova J, Sebela M, Beres T, Hluska T, Smehilova M, Bilyeu KD, Frebort I (2010)
611 Vacuolar and cytosolic cytokinin dehydrogenases of Arabidopsis thaliana: heterologous expression,
612 purification and properties. Phytochemistry 71: 1970-1978
613 Kudo T, Makita N, Kojima M, Tokunaga H, Sakakibara H (2012) Cytokinin activity of cis-zeatin and phenotypic
614 alterations induced by overexpression of putative cis-Zeatin-O-glucosyltransferase in rice. Plant Physiol
615 160: 319-331
616 Kumar S, Stecher G, Li M, Knyaz C, Tamura K (2018) MEGA X: Molecular Evolutionary Genetics Analysis

across Computing Platforms. Mol Biol Evol 35: 1547-1549

Kurakawa T, Ueda N, Maekawa M, Kobayashi K, Kojima M, Nagato Y, Sakakibara H, Kyozuka J (2007) Direct control of shoot meristem activity by a cytokinin-activating enzyme. Nature 445: 652-655

Li S, Zhao B, Yuan D, Duan M, Qian Q, Tang L, Wang B, Liu X, Zhang J, Wang J, Sun J, Liu Z, Feng YQ, Yuan L, Li C (2013) Rice zinc finger protein DST enhances grain production through controlling Gn1a/OsCKX2 expression. Proc Natl Acad Sci U S A 110: 3167-3172

Madeira F, Park YM, Lee J, Buso N, Gur T, Madhusoodanan N, Basutkar P, Tivey ARN, Potter SC, Finn RD, Lopez R (2019) The EMBL-EBI search and sequence analysis tools APIs in 2019. Nucleic Acids Res 47: W636-W641

Mao C, He J, Liu L, Deng Q, Yao X, Liu C, Qiao Y, Li P, Ming F (2020) OsNAC2 integrates auxin and cytokinin pathways to modulate rice root development. Plant Biotechnol J 18: 429-442

Mao Y, Zhang H, Xu N, Zhang B, Gou F, Zhu JK (2013) Application of the CRISPR-Cas system for efficient genome engineering in plants. Mol Plant 6: 2008-2011

Niemann MCE, Weber H, Hluska T, Leonte G, Anderson SM, Novak O, Senes A, Werner T (2018) The Cytokinin Oxidase/Dehydrogenase CKX1 Is a Membrane-Bound Protein Requiring Homooligomerization in the Endoplasmic Reticulum for Its Cellular Activity. Plant Physiol 176: 2024-2039

Osugi A, Kojima M, Takebayashi Y, Ueda N, Kiba T, Sakakibara H (2017) Systemic transport of trans-zeatin and its precursor have differing roles in Arabidopsis shoots. Nat Plants 3: 17112

Romanov GA, Schmulling T (2021) Opening Doors for Cytokinin Trafficking at the ER Membrane. Trends Plant Sci

Sakamoto T, Sakakibara H, Kojima M, Yamamoto Y, Nagasaki H, Inukai Y, Sato Y, Matsuoka M (2006) Ectopic expression of KNOTTED1-like homeobox protein induces expression of cytokinin biosynthesis genes in rice. Plant Physiol 142: 54-62

Schwarz I, Scheirlinck MT, Otto E, Bartrina I, Schmidt RC, Schmulling T (2020) Cytokinin regulates the activity of the inflorescence meristem and components of seed yield in oilseed rape. J Exp Bot

Shin SY, Jeong JS, Lim JY, Kim T, Park JH, Kim JK, Shin C (2018) Transcriptomic analyses of rice (Oryza sativa) genes and non-coding RNAs under nitrogen starvation using multiple omics technologies. BMC Genomics 19: 532

Simaskova M, O'Brien JA, Khan M, Van Noorden G, Otvos K, Vieten A, De Clercq I, Van Haperen JMA, Cuesta C, Hoyerova K, Vanneste S, Marhavy P, Wabnik K, Van Breusegem F, Nowack M, Murphy A, Friml J, Weijers D, Beeckman T, Benkova E (2015) Cytokinin response factors regulate PIN-FORMED auxin transporters. Nat Commun 6: 8717

Takeda T, Suwa Y, Suzuki M, Kitano H, Ueguchi-Tanaka M, Ashikari M, Matsuoka M, Ueguchi C (2003) The OsTB1 gene negatively regulates lateral branching in rice. Plant J 33: 513-520

Tezuka D, Ito A, Mitsuhashi W, Toyomasu T, Imai R (2015) The rice ent-KAURENE SYNTHASE LIKE 2 encodes a functional ent-beyerene synthase. Biochem Biophys Res Commun 460: 766-771

Tsai YC, Weir NR, Hill K, Zhang W, Kim HJ, Shiu SH, Schaller GE, Kieber JJ (2012) Characterization of genes involved in cytokinin signaling and metabolism from rice. Plant Physiol 158: 1666-1684

Waldie T, Leyser O (2018) Cytokinin Targets Auxin Transport to Promote Shoot Branching. Plant Physiol 177: 803-818

Wang J, Xu H, Li N, Fan F, Wang L, Zhu Y, Li S (2015) Artificial Selection of Gn1a Plays an Important role in Improving Rice Yields Across Different Ecological Regions. Rice (N Y) 8: 37

Wang WC, Lin TC, Kieber J, Tsai YC (2019) Response Regulators 9 and 10 Negatively Regulate Salinity

Tolerance in Rice. Plant Cell Physiol 60: 2549-2563

Wang Y, Lu Y, Guo Z, Ding Y, Ding C (2020) RICE CENTRORADIALIS 1, a TFL1-like Gene, Responses to Drought Stress and Regulates Rice Flowering Transition. Rice (N Y) 13: 70

Werner T, Motyka V, Strnad M, Schmulling T (2001) Regulation of plant growth by cytokinin. Proc Natl Acad Sci U S A 98: 10487-10492

Xu J, Zha M, Li Y, Ding Y, Chen L, Ding C, Wang S (2015) The interaction between nitrogen availability and auxin, cytokinin, and strigolactone in the control of shoot branching in rice (Oryza sativa L.). Plant Cell Rep 34: 1647-1662

Yang J, Cho LH, Yoon J, Yoon H, Wai AH, Hong WJ, Han M, Sakakibara H, Liang W, Jung KH, Jeon JS, Koh HJ, Zhang D, An G (2018) Chromatin interacting factor OsVIL2 increases biomass and rice grain yield. Plant Biotechnol J

Yeh SY, Chen HW, Ng CY, Lin CY, Tseng TH, Li WH, Ku MS (2015) Down-Regulation of Cytokinin Oxidase 2 Expression Increases Tiller Number and Improves Rice Yield. Rice (N Y) 8: 36

Yu C, Liu Y, Zhang A, Su S, Yan A, Huang L, Ali I, Liu Y, Forde BG, Gan Y (2015) MADS-box transcription factor OsMADS25 regulates root development through affection of nitrate accumulation in rice. PLoS One 10: e0135196

Zalabak D, Galuszka P, Mrizova K, Podlesakova K, Gu R, Frebortova J (2014) Biochemical characterization of the maize cytokinin dehydrogenase family and cytokinin profiling in developing maize plantlets in relation to the expression of cytokinin dehydrogenase genes. Plant Physiol Biochem 74: 283-293

Zalabak D, Johnova P, Plihal O, Senkova K, Samajova O, Jiskrova E, Novak O, Jackson D, Mohanty A, Galuszka P (2016) Maize cytokinin dehydrogenase isozymes are localized predominantly to the vacuoles. Plant Physiol Biochem 104: 114-124

Zalewski W, Galuszka P, Gasparis S, Orczyk W, Nadolska-Orczyk A (2010) Silencing of the HvCKX1 gene decreases the cytokinin oxidase/dehydrogenase level in barley and leads to higher plant productivity. J Exp Bot 61: 1839-1851

Zhang L, Zhao YL, Gao LF, Zhao GY, Zhou RH, Zhang BS, Jia JZ (2012) TaCKX6-D1, the ortholog of rice OsCKX2, is associated with grain weight in hexaploid wheat. New Phytol 195: 574-584

Zhang W, Peng KX, Cui FB, Wang DL, Zhao JZ, Zhang YJ, Yu NN, Wang YY, Zeng DL, Wang YH, Cheng ZK, Zhang KW (2020) Cytokinin oxidase/dehydrogenase OsCKX11 coordinates source and sink relationship in rice by simultaneous regulation of leaf senescence and grain number. Plant Biotechnology Journal

Zhao Y, Hu Y, Dai M, Huang L, Zhou DX (2009) The WUSCHEL-related homeobox gene WOX11 is required to activate shoot-borne crown root development in rice. Plant Cell 21: 736-748

Zou J, Chen Z, Zhang S, Zhang W, Jiang G, Zhao X, Zhai W, Pan X, Zhu L (2005) Characterizations and fine mapping of a mutant gene for high tillering and dwarf in rice (Oryza sativa L.). Planta 222: 604-612

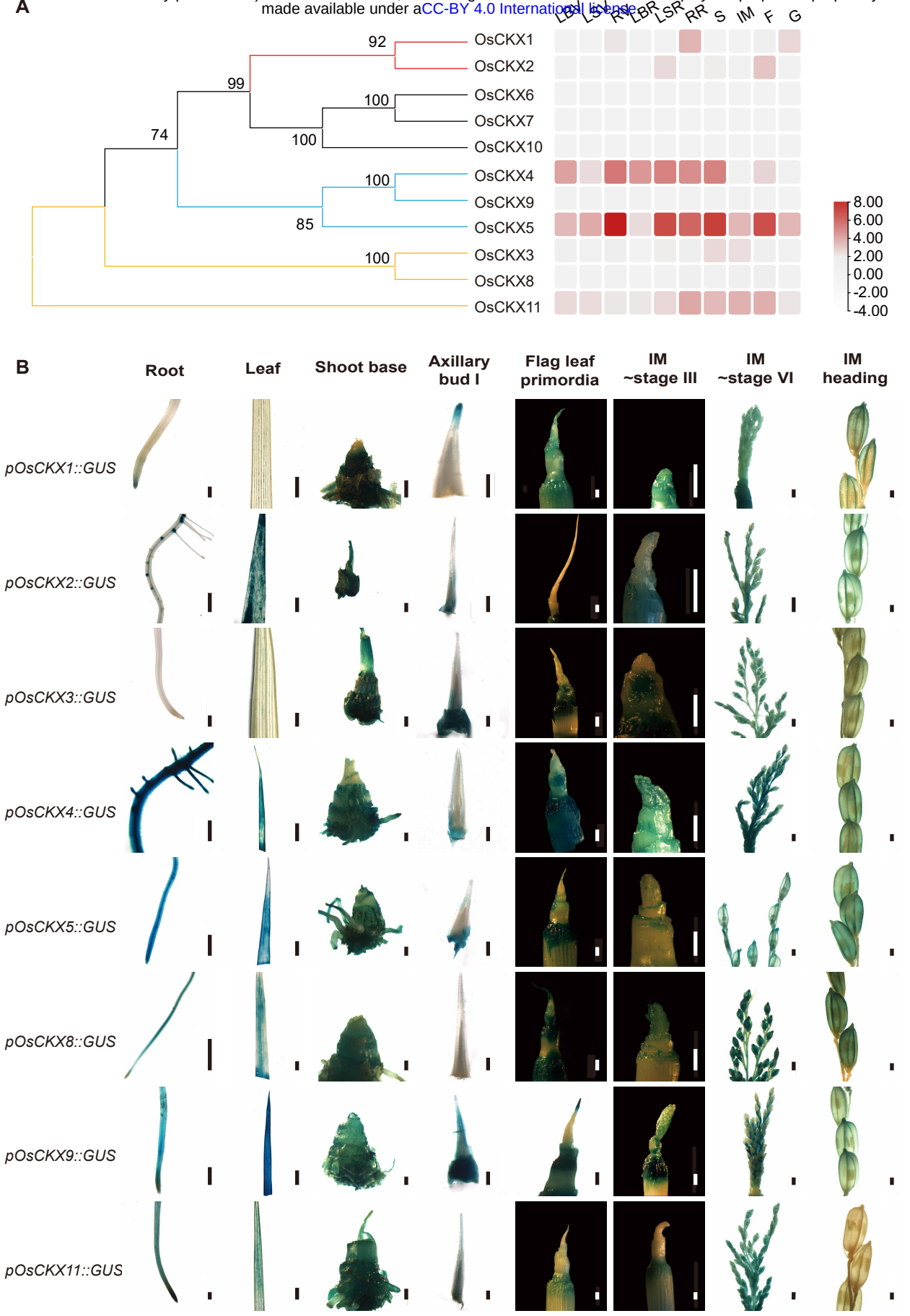

Figure 1. Genetic relationship and expression patterns of *OsCKX* genes based on RNA sequencing data and GUS staining assay. A, Genetic relationship and expression patterns of *OsCKX* genes investigated in the leaf blade at the vegetative stage (LBV), leaf sheath at the vegetative stage (LSV), root at the vegetative stage (RV), leaf blade at the reproductive stage (LBR), leaf sheath at the reproductive stage (LSR), root at the reproductive stage (RR), stem (S), inflorescence meristem (IM), flower (F), and grain (G). The expression pattern was based on $\log_2$ Fragments Per Kilobase of exon model per Million mapped fragments (FPKM) values. B, Histochemical GUS staining of *pOsCKX::GUS* transgenic plants at various developmental stages. The scale bar in B was 1 mm.

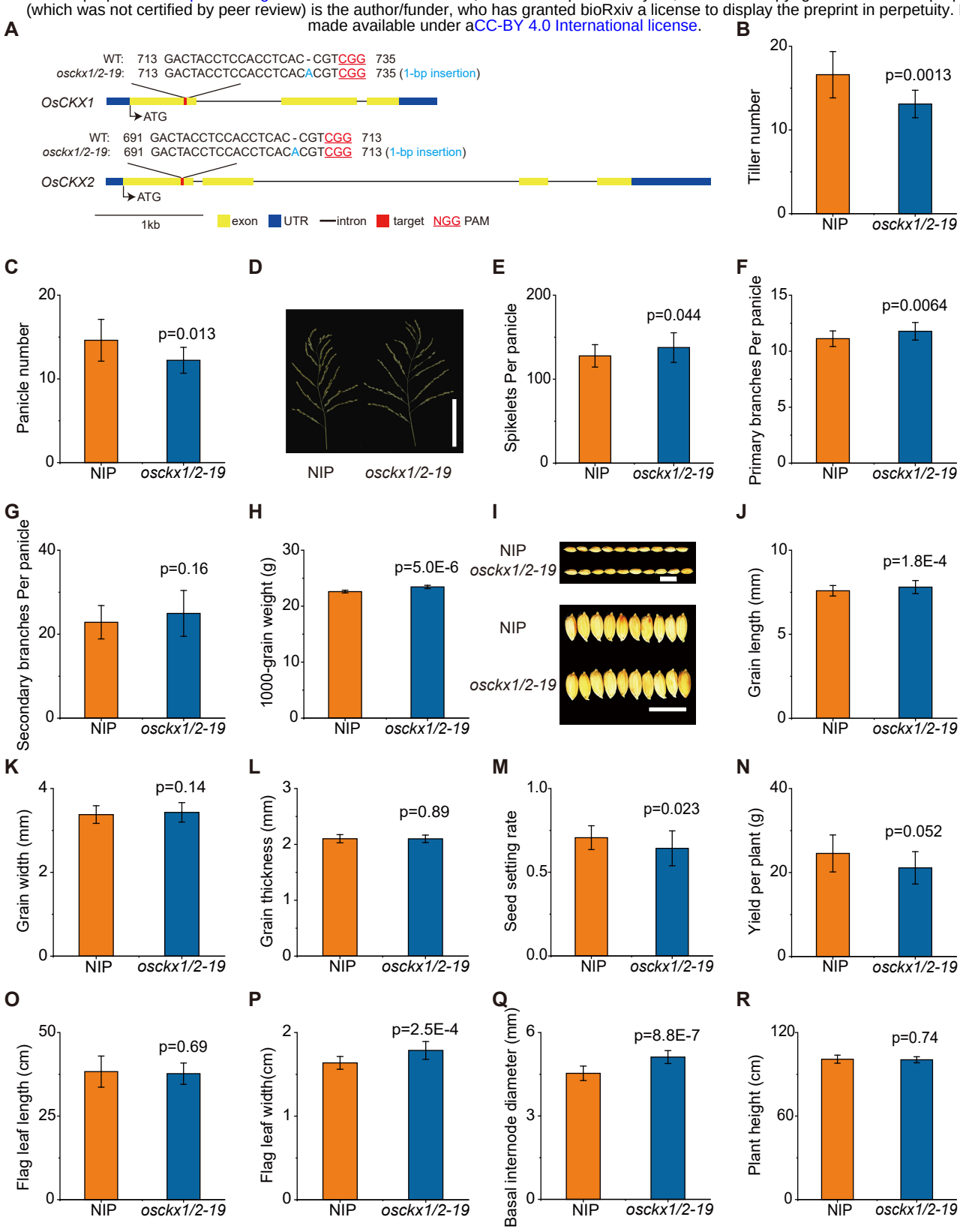

Figure 2. Genetic and phenotypic characterization between wild-type (WT) and *osckx1/2-19* mutant plants. A, Mutation details of the coding sequences in the *OsCKX1* and *OsCKX2* of *osckx1/2-19* mutant. Both *OsCKX1* and *OsCKX2* had functional loss due to the 1-bp insertion caused by frameshift mutation. The solid yellow, blue, and red boxes represent the exons, untranslated regions, and target sequences, respectively. The introns are shown as solid lines, while protospacer adjacent motif (PAM) sequences are shown in red color and underlined with red. B, Number of tillers at the vegetative stage 70 days after sowing. C, Panicles at the reproductive stage (n = 20 for Nipponbare [NIP], n = 10 for *osckx1/2-19*). D, Panicle phenotypes of NIP and *osckx1/2-19* plants. The image was digitally extracted and scaled for comparison (scale bar = 10 cm). E–H, Measurement of the spikelets per panicle (E), primary branches per panicle (F), secondary branches per panicle (G), 1,000-grain weight (H) (n > 20 for E–G, n = 5 for H) and *osckx1/2-19* (n > 10 for E–G, n = 5 for H) plants. I, Grain phenotypes of NIP and *osckx1/2-19* plants. The image was digitally extracted and scaled for comparison (scale bar = 1 cm). J-R, Measurement of the grain length (J), grain weight (K), and grain thickness (L) , seed setting rate (M), yield per plant (N), length of flag leaves (O), width of flag leaves (P), basal internode diameter (Q), and plant height (R) of NIP (n > 50 for J–L, n > 20 for M–Q) and *osckx1/2-19* ((n > 50 for J–L, n > 10 for M–Q) plants. The P-values indicate the significant differences between NIP and *osckx1/2-19* determined by Student's *t*-test.

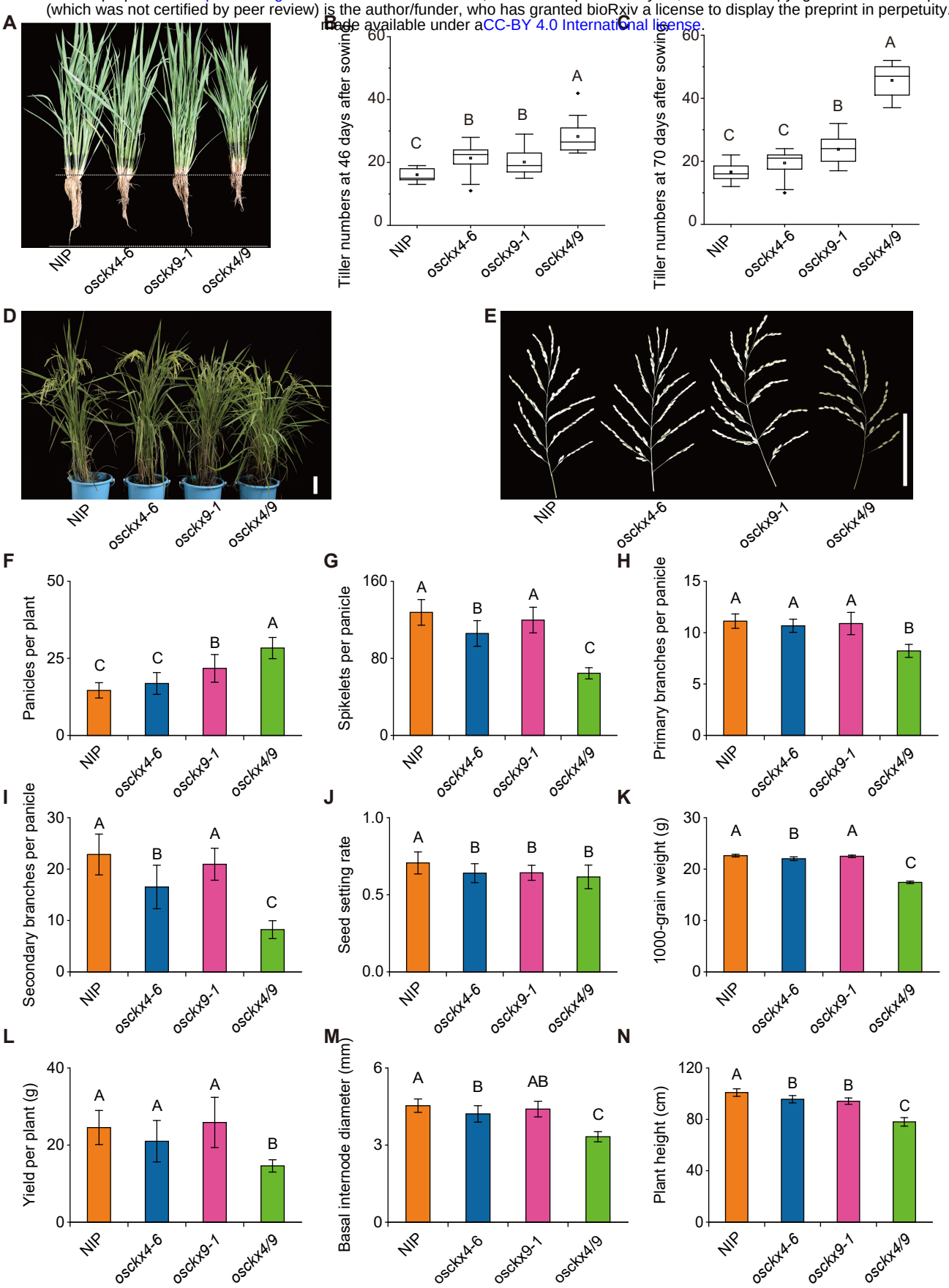

Figure 3. Phenotypic characterization between wild-type (WT) and *osckx4*, *osckx9*, and *osckx4/9* mutant plants from the field experiment. A, Phenotypic features of Nipponbare (NIP), *osckx4-6*, *osckx9-1* and *osckx4/9* seedlings at the vegetative stage 46 days after sowing. The image was digitally extracted and scaled for comparison (scale bar = 10 cm). B–C, Number of tillers at the vegetative stage 46 days after sowing (B) and reproductive stage 70 days after sowing (C) (n > 20 for NIP, *osckx4-6*, and *osckx9-1*, n = 10 for *osckx4/9*). D–E, Habits (D) and panicle phenotypes (E) of NIP, *osckx4-6*, *osckx9-1*, and *osckx4/9* plants at the mature stage. The image was digitally extracted and scaled for comparison (scale bar = 10 cm). F–N, Measurement of the panicle number (F), spikelets per panicle (G), seed setting rate (H), 1,000-grain weight (I), yield per plant (J), plant height (K), primary branches per panicle (L), secondary branches per panicle (M), and diameter of basal internode of NIP (N), *osckx4-6*, *osckx9-1* (n > 20 for F–H and J–N, n = 5 for I), and *osckx4/9* (n > 10 for F–H and J–N, n = 5 for I). Different capital letters represent significant differences ($P < 0.01$) determined by one-way ANOVA and shortest significant ranges (SSR) test.

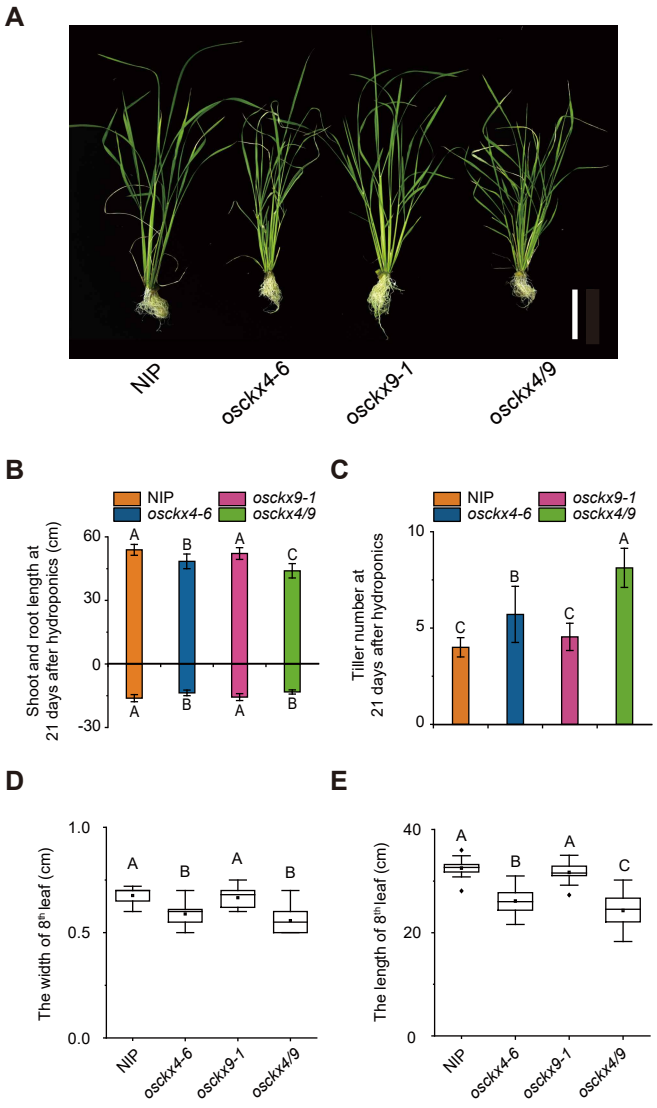

Figure 4. Phenotypic characterization between wild-type (WT) and *osckx4*, *osckx9*, and *osckx4/9* mutant plants from the hydroponic experiment. A, Phenotypic features of Nipponbare (NIP), *osckx4-6*, *osckx9-1*, and *osckx4/9* seedlings 21 days after transferring to hydroponic solutions. The image was digitally extracted and scaled for comparison (scale bar = 10 cm). B–E, Measurement of the shoot and root lengths (B), tiller numbers (C), length of 8th leaf (D), and width of 8th leaf (E) of NIP, *osckx4-6*, *osckx9-1*, and *osckx4/9* seedlings (n = 24 each). Different capital letters represent significant differences ($P < 0.01$) determined by one-way ANOVA and SSR test.

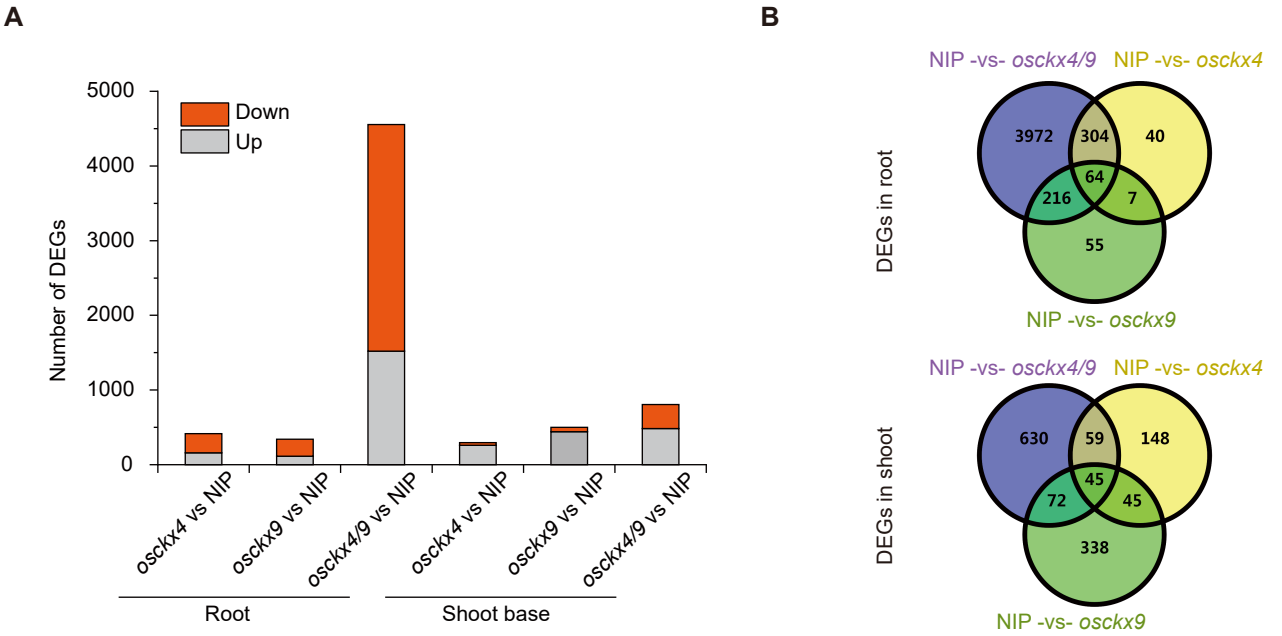

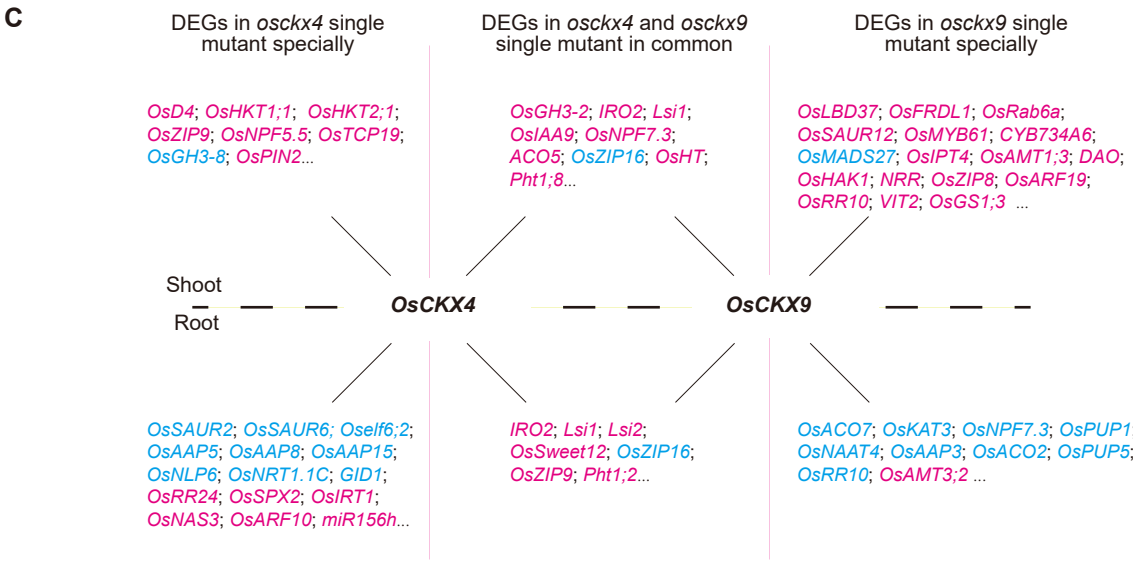

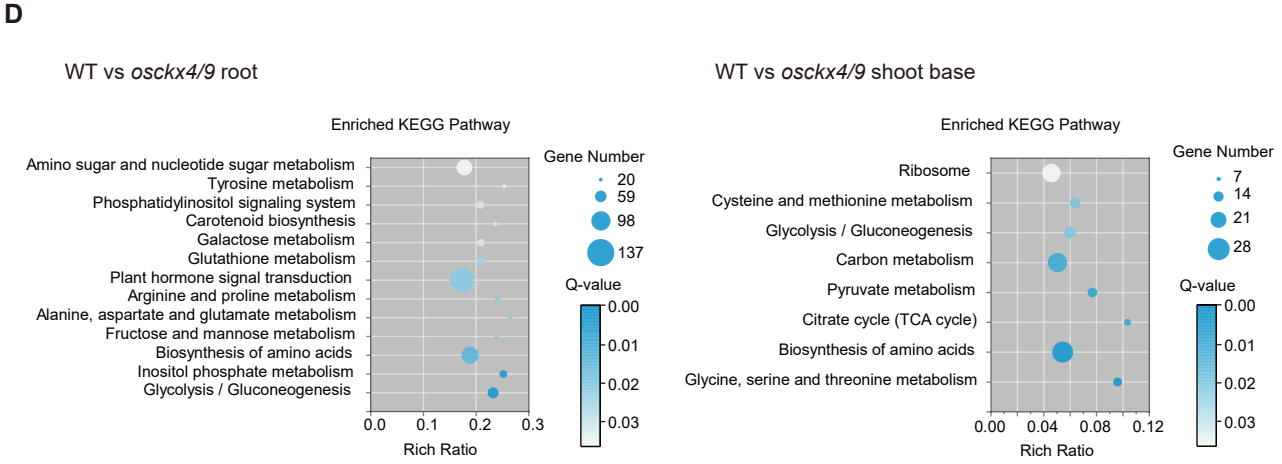

Figure 5. RNA-seq analysis of the roots and shoot bases (BP) between wild-type (WT) and *osckx4*, *osckx9*, and *osckx4/9* mutant plants. A, The number of differentially expressed genes (DEGs) identified in the roots and shoot bases of the following pairwise comparisons: Nipponbare (NIP) vs. *osckx4*, NIP vs. *osckx9*, and NIP vs. *osckx4/9*. The changes in gene expression levels were calculated using the $\log_2$ fold change and Q values from three biological replicates. B, Overlapping DEGs in the roots and shoot bases (BP) of NIP vs. *osckx4*, NIP vs. *osckx9*, and NIP vs. *osckx4/9*. C, DEGs in *osckx4* and *osckx9* specifically and in commonin the roots and shoots, genes in magenta are upregulated; genes in sky blue are down-regulated. D, Top enriched Kyoto Encyclopedia of Genes and Genomes (KEGG) pathways of the DEGs identified in the roots and shoot bases of NIP vs. *osckx4/9*.

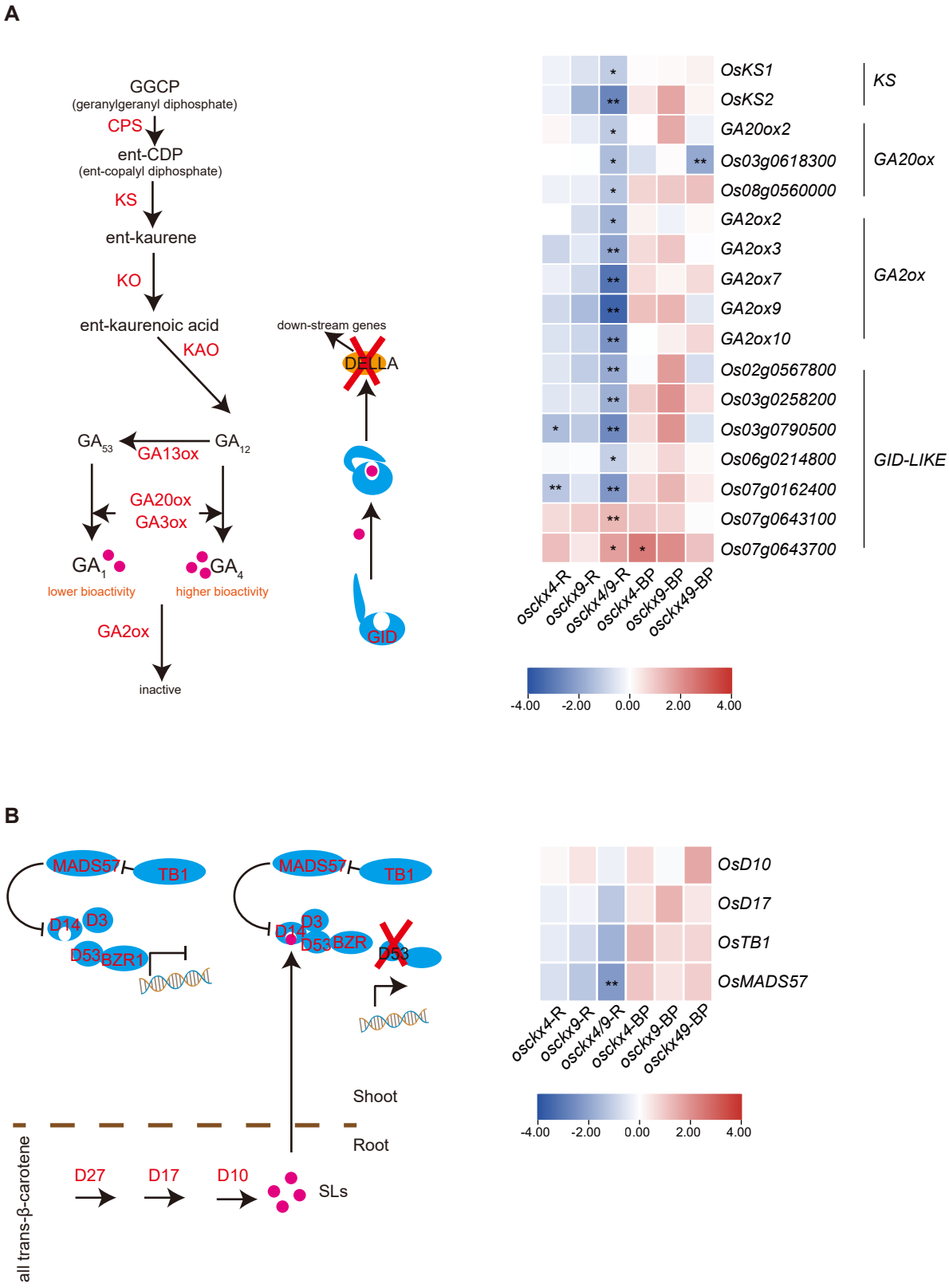

Figure 6. *OsCKX4* and *OsCKX9* are associated with several signal transduction pathways. A, Differentially expressed genes (DEGs) related to gibberellin metabolism and signaling transduction. B, DEGs related to strigolactone biosynthesis and signaling transduction. * Q < 0.05, ** Q < 0.01.

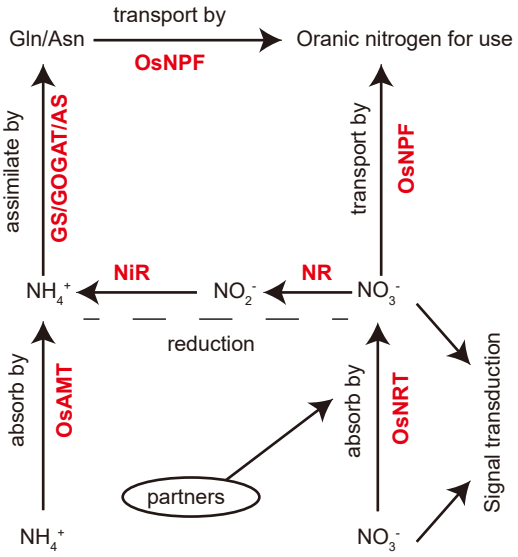

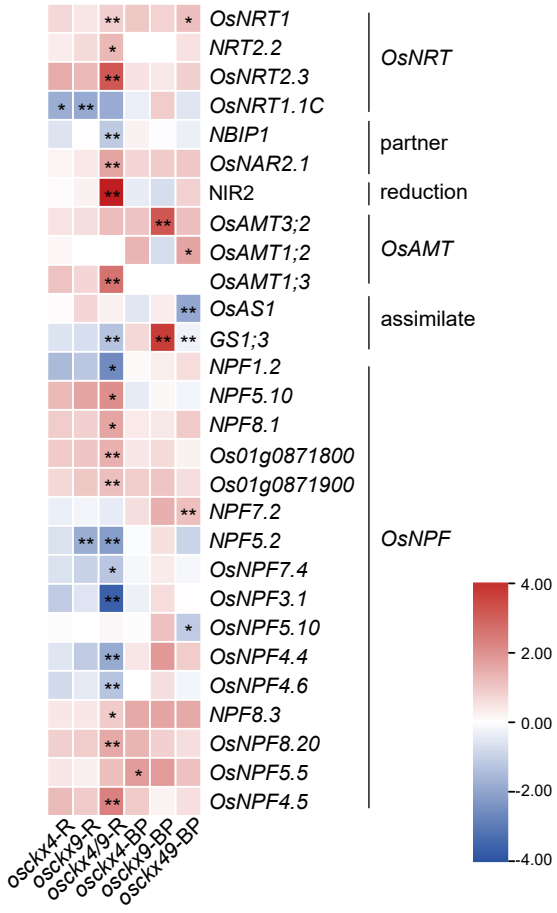

Figure 7. *OsCKX4* and *OsCKX9* associated with nitrogen absorption. Differentially expressed genes related to nitrogen absorption, metabolism, and transportation. * Q < 0.05, ** Q < 0.01.

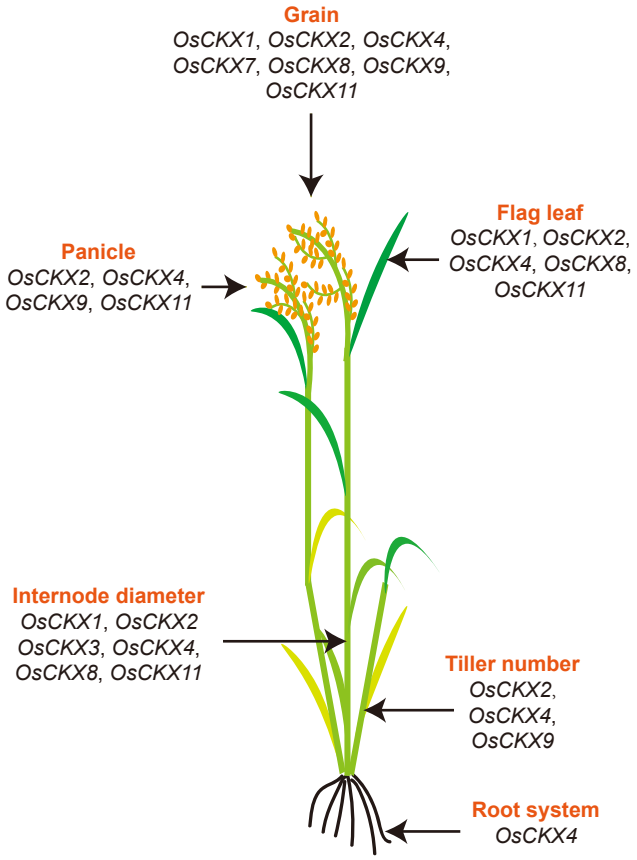

Figure 8. Patterns of *OsCKX* genes in rice.

Parsed Citations

Arite T, Iwata H, Ohshima K, Maekawa M, Nakajima M, Kojima M, Sakakibara H, Kyozuka J (2007) DWARF10, an RMS1/MAX4/DAD1 ortholog, controls lateral bud outgrowth in rice. Plant J 51: 1019-1029
Google Scholar: Author Only Title Only Author and Title

Ashikari M, Sakakibara H, Lin S, Yamamoto T, Takashi T, Nishimura A, Angeles ER, Qian Q, Kitano H, Matsuoka M (2005) Cytokinin oxidase regulates rice grain production. Science 309: 741-745
Google Scholar: Author Only Title Only Author and Title

Bartrina I, Otto E, Strnad M, Werner T, Schmulling T (2011) Cytokinin regulates the activity of reproductive meristems, flower organ size, ovule formation, and thus seed yield in Arabidopsis thaliana. Plant Cell 23: 69-80
Google Scholar: Author Only Title Only Author and Title

Chen L, Zhao J, Song J, Jameson PE (2020) Cytokinin dehydrogenase: a genetic target for yield improvement in wheat. Plant Biotechnol J 18: 614-630
Google Scholar: Author Only Title Only Author and Title

Chen Y, Fan X, Song W, Zhang Y, Xu G (2012) Over-expression of OsPIN2 leads to increased tiller numbers, angle and shorter plant height through suppression of OsLAZY1. Plant Biotechnol J 10: 139-149
Google Scholar: Author Only Title Only Author and Title

Ding C, You J, Chen L, Wang S, Ding Y (2014) Nitrogen fertilizer increases spikelet number per panicle by enhancing cytokinin synthesis in rice. Plant Cell Rep 33: 363-371
Google Scholar: Author Only Title Only Author and Title

Duan J, Yu H, Yuan K, Liao Z, Meng X, Jing Y, Liu G, Chu J, Li J (2019) Strigolactone promotes cytokinin degradation through transcriptional activation of CYTOKININ OXIDASE/DEHYDROGENASE 9 in rice. Proc Natl Acad Sci U S A 116: 14319-14324
Google Scholar: Author Only Title Only Author and Title

Gao S, Fang J, Xu F, Wang W, Sun X, Chu J, Cai B, Feng Y, Chu C (2014) CYTOKININ OXIDASE/DEHYDROGENASE4 Integrates Cytokinin and Auxin Signaling to Control Rice Crown Root Formation. Plant Physiol 165: 1035-1046
Google Scholar: Author Only Title Only Author and Title

Gao S, Xiao Y, Xu F, Gao X, Cao S, Zhang F, Wang G, Sanders D, Chu C (2019) Cytokinin-dependent regulatory module underlies the maintenance of zinc nutrition in rice. New Phytol 224: 202-215
Google Scholar: Author Only Title Only Author and Title

Guo S, Xu Y, Liu H, Mao Z, Zhang C, Ma Y, Zhang Q, Meng Z, Chong K (2013) The interaction between OsMADS57 and OsTB1 modulates rice tillering via DWARF14. Nat Commun 4: 1566
Google Scholar: Author Only Title Only Author and Title

Jameson PE, Song J (2020) Will cytokinins underpin the second 'Green Revolution'? J Exp Bot 71: 6872-6875
Google Scholar: Author Only Title Only Author and Title

Ji SH, Gururani MA, Lee JW, Ahn BO, Chun SC (2014) Isolation and characterisation of a dwarf rice mutant exhibiting defective gibberellins biosynthesis. Plant Biol (Stuttg) 16: 428-439
Google Scholar: Author Only Title Only Author and Title

Joshi R, Sahoo KK, Tripathi AK, Kumar R, Gupta BK, Pareek A, Singla-Pareek SL (2018) Knockdown of an inflorescence meristem-specific cytokinin oxidase - OsCKX2 in rice reduces yield penalty under salinity stress condition. Plant Cell Environ 41: 936-946
Google Scholar: Author Only Title Only Author and Title

Kanehisa M (2019) Toward understanding the origin and evolution of cellular organisms. Protein Science 28: 1947-1951
Google Scholar: Author Only Title Only Author and Title

Kollmer I, Novak O, Strnad M, Schmulling T, Werner T (2014) Overexpression of the cytosolic cytokinin oxidase/dehydrogenase (CKX7) from Arabidopsis causes specific changes in root growth and xylem differentiation. Plant J 78: 359-371
Google Scholar: Author Only Title Only Author and Title

Kowalska M, Galuszka P, Frebortova J, Sebela M, Beres T, Hluska T, Smehilova M, Bilyeu KD, Frebort I (2010) Vacuolar and cytosolic cytokinin dehydrogenases of Arabidopsis thaliana: heterologous expression, purification and properties. Phytochemistry 71: 1970-1978
Google Scholar: Author Only Title Only Author and Title

Kudo T, Makita N, Kojima M, Tokunaga H, Sakakibara H (2012) Cytokinin activity of cis-zeatin and phenotypic alterations induced by overexpression of putative cis-Zeatin-O-glucosyltransferase in rice. Plant Physiol 160: 319-331
Google Scholar: Author Only Title Only Author and Title

Kumar S, Stecher G, Li M, Knyaz C, Tamura K (2018) MEGA X: Molecular Evolutionary Genetics Analysis across Computing Platforms. Mol Biol Evol 35: 1547-1549
Google Scholar: Author Only Title Only Author and Title

Kurakawa T, Ueda N, Maekawa M, Kobayashi K, Kojima M, Nagato Y, Sakakibara H, Kyozuka J (2007) Direct control of shoot meristem

activity by a cytokinin-activating enzyme. Nature 445: 652-655
Google Scholar: Author Only Title Only Author and Title

Li S, Zhao B, Yuan D, Duan M, Qian Q, Tang L, Wang B, Liu X, Zhang J, Wang J, Sun J, Liu Z, Feng YQ, Yuan L, Li C (2013) Rice zinc finger protein DST enhances grain production through controlling Gn1a/OsCKX2 expression. Proc Natl Acad Sci U S A 110: 3167-3172
Google Scholar: Author Only Title Only Author and Title

Madeira F, Park YM, Lee J, Buso N, Gur T, Madhusoodanan N, Basutkar P, Tivey ARN, Potter SC, Finn RD, Lopez R (2019) The EMBL-EBI search and sequence analysis tools APIs in 2019. Nucleic Acids Res 47: W636-W641
Google Scholar: Author Only Title Only Author and Title

Mao C, He J, Liu L, Deng Q, Yao X, Liu C, Qiao Y, Li P, Ming F (2020) OsNAC2 integrates auxin and cytokinin pathways to modulate rice root development. Plant Biotechnol J 18: 429-442
Google Scholar: Author Only Title Only Author and Title

Mao Y, Zhang H, Xu N, Zhang B, Gou F, Zhu JK (2013) Application of the CRISPR-Cas system for efficient genome engineering in plants. Mol Plant 6: 2008-2011
Google Scholar: Author Only Title Only Author and Title

Niemann MCE, Weber H, Hluska T, Leonte G, Anderson SM, Novak O, Senes A, Werner T (2018) The Cytokinin Oxidase/Dehydrogenase CKX1 Is a Membrane-Bound Protein Requiring Homooligomerization in the Endoplasmic Reticulum for Its Cellular Activity. Plant Physiol 176: 2024-2039
Google Scholar: Author Only Title Only Author and Title

Osugi A, Kojima M, Takebayashi Y, Ueda N, Kiba T, Sakakibara H (2017) Systemic transport of trans-zeatin and its precursor have differing roles in Arabidopsis shoots. Nat Plants 3: 17112
Google Scholar: Author Only Title Only Author and Title

Romanov GA, Schmulling T (2021) Opening Doors for Cytokinin Trafficking at the ER Membrane. Trends Plant Sci
Google Scholar: Author Only Title Only Author and Title

Sakamoto T, Sakakibara H, Kojima M, Yamamoto Y, Nagasaki H, Inukai Y, Sato Y, Matsuoka M (2006) Ectopic expression of KNOTTED1-like homeobox protein induces expression of cytokinin biosynthesis genes in rice. Plant Physiol 142: 54-62
Google Scholar: Author Only Title Only Author and Title

Schwarz I, Scheirlinck MT, Otto E, Bartrina I, Schmidt RC, Schmulling T (2020) Cytokinin regulates the activity of the inflorescence meristem and components of seed yield in oilseed rape. J Exp Bot
Google Scholar: Author Only Title Only Author and Title

Shin SY, Jeong JS, Lim JY, Kim T, Park JH, Kim JK, Shin C (2018) Transcriptomic analyses of rice (Oryza sativa) genes and non-coding RNAs under nitrogen starvation using multiple omics technologies. BMC Genomics 19: 532
Google Scholar: Author Only Title Only Author and Title

Simaskova M, O'Brien JA, Khan M, Van Noorden G, Otvos K, Vieten A, De Clercq I, Van Haperen JMA, Cuesta C, Hoyerova K, Vanneste S, Marhavy P, Wabnik K, Van Breusegem F, Nowack M, Murphy A, Friml J, Weijers D, Beeckman T, Benkova E (2015) Cytokinin response factors regulate PIN-FORMED auxin transporters. Nat Commun 6: 8717
Google Scholar: Author Only Title Only Author and Title

Takeda T, Suwa Y, Suzuki M, Kitano H, Ueguchi-Tanaka M, Ashikari M, Matsuoka M, Ueguchi C (2003) The OsTB1 gene negatively regulates lateral branching in rice. Plant J 33: 513-520
Google Scholar: Author Only Title Only Author and Title

Tezuka D, Ito A, Mitsuhashi W, Toyomasu T, Imai R (2015) The rice ent-KAURENE SYNTHASE LIKE 2 encodes a functional ent-beyerene synthase. Biochem Biophys Res Commun 460: 766-771
Google Scholar: Author Only Title Only Author and Title

Tsai YC, Weir NR, Hill K, Zhang W, Kim HJ, Shiu SH, Schaller GE, Kieber JJ (2012) Characterization of genes involved in cytokinin signaling and metabolism from rice. Plant Physiol 158: 1666-1684
Google Scholar: Author Only Title Only Author and Title

Waldie T, Leyser O (2018) Cytokinin Targets Auxin Transport to Promote Shoot Branching. Plant Physiol 177: 803-818
Google Scholar: Author Only Title Only Author and Title

Wang J, Xu H, Li N, Fan F, Wang L, Zhu Y, Li S (2015) Artificial Selection of Gn1a Plays an Important role in Improving Rice Yields Across Different Ecological Regions. Rice (N Y) 8: 37
Google Scholar: Author Only Title Only Author and Title

Wang WC, Lin TC, Kieber J, Tsai YC (2019) Response Regulators 9 and 10 Negatively Regulate Salinity Tolerance in Rice. Plant Cell Physiol 60: 2549-2563
Google Scholar: Author Only Title Only Author and Title

Wang Y, Lu Y, Guo Z, Ding Y, Ding C (2020) RICE CENTRORADIALIS 1, a TFL1-like Gene, Responses to Drought Stress and Regulates Rice Flowering Transition. Rice (N Y) 13: 70
Google Scholar: Author Only Title Only Author and Title

Werner T, Motyka V, Strnad M, Schmulling T (2001) Regulation of plant growth by cytokinin. Proc Natl Acad Sci U S A 98: 10487-10492
Google Scholar: Author Only Title Only Author and Title

Xu J, Zha M, Li Y, Ding Y, Chen L, Ding C, Wang S (2015) The interaction between nitrogen availability and auxin, cytokinin, and strigolactone in the control of shoot branching in rice (Oryza sativa L.). Plant Cell Rep 34: 1647-1662
Google Scholar: Author Only Title Only Author and Title

Yang J, Cho LH, Yoon J, Yoon H, Wai AH, Hong WJ, Han M, Sakakibara H, Liang W, Jung KH, Jeon JS, Koh HJ, Zhang D, An G (2018) Chromatin interacting factor OsVIL2 increases biomass and rice grain yield. Plant Biotechnol J
Google Scholar: Author Only Title Only Author and Title

Yeh SY, Chen HW, Ng CY, Lin CY, Tseng TH, Li WH, Ku MS (2015) Down-Regulation of Cytokinin Oxidase 2 Expression Increases Tiller Number and Improves Rice Yield. Rice (N Y) 8: 36
Google Scholar: Author Only Title Only Author and Title

Yu C, Liu Y, Zhang A, Su S, Yan A, Huang L, Ali I, Liu Y, Forde BG, Gan Y (2015) MADS-box transcription factor OsMADS25 regulates root development through affection of nitrate accumulation in rice. PLoS One 10: e0135196
Google Scholar: Author Only Title Only Author and Title

Zalabak D, Galuszka P, Mrizova K, Podlesakova K, Gu R, Frebortova J (2014) Biochemical characterization of the maize cytokinin dehydrogenase family and cytokinin profiling in developing maize plantlets in relation to the expression of cytokinin dehydrogenase genes. Plant Physiol Biochem 74: 283-293
Google Scholar: Author Only Title Only Author and Title

Zalabak D, Johnova P, Plihal O, Senkova K, Samajova O, Jiskrova E, Novak O, Jackson D, Mohanty A, Galuszka P (2016) Maize cytokinin dehydrogenase isozymes are localized predominantly to the vacuoles. Plant Physiol Biochem 104: 114-124
Google Scholar: Author Only Title Only Author and Title

Zalewski W, Galuszka P, Gasparis S, Orczyk W, Nadolska-Orczyk A (2010) Silencing of the HvCKX1 gene decreases the cytokinin oxidase/dehydrogenase level in barley and leads to higher plant productivity. J Exp Bot 61: 1839-1851
Google Scholar: Author Only Title Only Author and Title

Zhang L, Zhao YL, Gao LF, Zhao GY, Zhou RH, Zhang BS, Jia JZ (2012) TaCKX6-D1, the ortholog of rice OsCKX2, is associated with grain weight in hexaploid wheat. New Phytol 195: 574-584
Google Scholar: Author Only Title Only Author and Title

Zhang W, Peng KX, Cui FB, Wang DL, Zhao JZ, Zhang YJ, Yu NN, Wang YY, Zeng DL, Wang YH, Cheng ZK, Zhang KW (2020) Cytokinin oxidase/dehydrogenase OsCKX11 coordinates source and sink relationship in rice by simultaneous regulation of leaf senescence and grain number. Plant Biotechnology Journal
Google Scholar: Author Only Title Only Author and Title

Zhao Y, Hu Y, Dai M, Huang L, Zhou DX (2009) The WUSCHEL-related homeobox gene WOX11 is required to activate shoot-borne crown root development in rice. Plant Cell 21: 736-748
Google Scholar: Author Only Title Only Author and Title

Zou J, Chen Z, Zhang S, Zhang W, Jiang G, Zhao X, Zhai W, Pan X, Zhu L (2005) Characterizations and fine mapping of a mutant gene for high tillering and dwarf in rice (Oryza sativa L.). Planta 222: 604-612
Google Scholar: Author Only Title Only Author and Title